Institut für Geodäsie und Geoinformation

Investigations of Quality Aspects in UAV-Based Laser Scanning for Agriculture and Deformation Monitoring

Dissertation

zur Erlangung des Grades

Doktor der Ingenieurwissenschaften (Dr.–Ing.)

der

Agrar-, Ernährungs- und Ingenieurwissenschaftlichen Fakultät

der

Rheinischen Friedrich–Wilhelms–Universität Bonn

vorgelegt von

M.Sc. Ansgar Dreier

aus Schwabmünchen

Bonn 2025

Referent:	Prof. Dr. Heiner Kuhlmann
Korreferent:	Prof. Dr. Hans-Berndt Neuner

Tag der mündlichen Prüfung: 01.04.2025

Angefertigt mit Genehmigung der Agrar-, Ernährungs- und Ingenieurwissenschaftlichen Fakultät der Universität Bonn

Investigations of Quality Aspects in UAV-Based Laser Scanning for Agriculture and Deformation Monitoring

Abstract

This dissertation investigates the quality of UAV-based laser scanning and its applications in agriculture and deformation monitoring. UAV-based laser scanning is a growing technology that integrates sensors such as GNSS (Global Navigation Satellite System), IMU (Inertial Measurement Unit) and a laser scanner to produce high-resolution georeferenced 3D point clouds. This technology is increasingly used across various fields, including mining, surveying, forestry, and agriculture, due to its flexibility, detailed data acquisition, and the benefit of direct georeferencing, eliminating the need for ground control points in many cases.

The quality of these point clouds is crucial, as errors in trajectory estimation, system calibration, and sensor performance can significantly impact the quality and, therefore, the potential use of data. This dissertation addresses the use in precision agriculture and deformation monitoring with different quality aspects.

The study is divided into four main objectives:

- Evaluation of Direct Georeferencing: This objective assesses the quality of point clouds produced by UAV-based laser scanning with a focus on direct georeferencing. Key aspects evaluated include point cloud noise, accuracy, precision of repeated measurements, and the impact of GNSS master stations. By analyzing various flight patterns, such as cross-flight and corridor mapping, this research aims to understand and improve the performance of direct georeferencing, providing insights into how these systems and processing can be improved for different applications.
- Quality Aspects of a Full-Waveform 2D Laser Scanner: The second objective examines the quality of the 2D laser scanner (RIEGL miniVUX-2UAV) used in UAV-based laser scanning systems. This part of the research evaluates important parameters such as range precision, rangefinder offset, resolution capability, and multi-target capability. The goal is to understand the impact of the laser scanner on the overall error budget of the scanning system, providing a detailed assessment of how the sensor performs with a focus on multi-target detection.
- Estimation of Structural Plant Traits: This part applies UAV-based laser scanning to precision agriculture, focusing on the estimation of wheat crop height and plant area index (PAI). A novel ground classification algorithm based on k-means clustering is introduced to differentiate between ground and crop points. This approach investigates the quality in terms of the accuracy of structural plant trait estimation, addressing challenges related to the small object size and spatial resolution.
- Deformation Analysis of Water Dams: The final objective investigates the use of UAV-based laser scanning for deformation monitoring of water dams. This addresses challenges in trajectory estimation, flight planning, and the unique measurement environment. The study highlights both the potential and limitations in terms of the quality of UAV-based scanning, particularly in GNSS-denied environments. A following instance segmentation algorithm for rubble masonry is developed to enhance deformation analysis, enabling comparisons between point clouds from different epochs.

Overall, it provides a comprehensive discussion of UAV-based laser scanning technology and its applications, offering valuable insights into the understanding of point cloud quality and its use in different fields.

Untersuchungen zu Qualitätsaspekten beim UAV-basiertem Laserscanning für die Landwirtschaft und die Deformationsüberwachung

Zusammenfassung

In dieser Dissertation werden die Qualität des UAV-basierten Laserscannings und seine Anwendungen in der Landwirtschaft und der Deformationsüberwachung untersucht. UAV-basiertes Laserscanning ist eine wachsende Technologie, die Sensoren wie GNSS (Global Navigation Satellite System), IMU (Inertial Measurement Unit) und einen Laserscanner integriert, um hochauflösende georeferenzierte 3D-Punktwolken zu erzeugen. Diese Technologie wird aufgrund ihrer Flexibilität, der detaillierten Datenerfassung und des Vorteils der direkten Georeferenzierung, die in vielen Fällen den Einsatz von Bodenkontrollpunkten überflüssig macht, zunehmend in verschiedenen Bereichen wie Bergbau, Vermessung, Forst- und Landwirtschaft eingesetzt.

Die Qualität dieser Punktwolken ist von entscheidender Bedeutung, da Abweichungen bei der Trajektorienschätzung, der Systemkalibrierung und der Sensorgenauigkeit die Qualität und damit die potenzielle Nutzung der Daten erheblich beeinträchtigen können. Diese Dissertation befasst sich mit dem Einsatz in der Landwirtschaft und der Deformationsüberwachung unter verschiedenen Qualitätsaspekten.

Die Arbeit ist in vier Hauptziele unterteilt:

- Bewertung der direkten Georeferenzierung: Dieses Ziel bewertet die Qualität von Punktwolken, die durch UAV-basiertes Laserscanning erzeugt wurden, wobei der Schwerpunkt auf der direkten Georeferenzierung liegt. Zu den wichtigsten Aspekten, die bewertet werden, gehören das Rauschen der Punktwolken, die Genauigkeit, die Präzision von Mehrfachmessungen und der Einfluss von GNSS-Masterstationen. Durch die Analyse verschiedener Flugmuster, wie z. B. Kreuz- und Korridorbefliegung, zielt diese Untersuchung darauf ab, die Leistung der direkten Georeferenzierung zu verstehen und zu verbessern, und gibt Einblicke, wie diese Systeme und die Verarbeitung für verschiedene Anwendungen verbessert werden können.
- Qualitätsaspekte eines Full-Waveform 2D-Laserscanners: Ein weiteres Ziel ist die Untersuchung der Qualität des 2D-Laserscanners (RIEGL miniVUX-2UAV), der in UAV-basierten Laserscanning-Systemen eingesetzt wird. In diesem Teil der Arbeit werden wichtige Parameter wie Streckenpräzision, das Auflösungsvermögen und Multitarget-Fähigkeit bewertet. Ziel ist es, die Auswirkungen des Laserscanners auf das gesamte Abweichungsbudget des Scanningsystems zu verstehen und eine detaillierte Bewertung der Leistung des Sensors mit Schwerpunkt auf der Erkennung mehrerer Ziele vorzunehmen.
- Schätzung von strukturellen Pflanzenmerkmalen: In diesem Teil wird das UAV-basierte Laserscanning im Bereich der Landwirtschaft angewandt, wobei der Schwerpunkt auf der Ableitung der Pflanzenhöhe und des Pflanzenflächenindex (PAI) von Weizen liegt. Ein neuer Bodenklassifizierungsalgorithmus auf der Grundlage von k-means Klassifikation wird eingeführt, um zwischen Boden- und Pflanzenpunkten zu unterscheiden. Mit dieser Untersuchung wird die Qualität in Bezug auf die Genauigkeit der Schätzung struktureller Pflanzenmerkmale untersucht, wobei die Herausforderungen im Zusammenhang mit der geringen Objektgröße und räumlichen Auflösung behandelt werden.
- Deformationsanalyse von Staudämmen: Das letzte Ziel ist die Untersuchung des Einsatzes von UAV-basiertem Laserscanning für die Deformationsüberwachung von Staudämmen. Dabei geht es um Herausforderungen bei der Trajektorienschätzung, der Flugplanung und der Messumgebung. Die Studie zeigt sowohl das Potenzial als auch die Grenzen der Qualität des UAV-basierten Laserscannings auf, insbesondere in Umgebungen, in denen schlechte GNSS Bedingungen vorliegen. Zur Verbesserung der Deformationsanalyse wird außerdem ein neuer Segmentierungsalgorithmus für Steine entwickelt, der Vergleiche zwischen Punktwolken aus verschiedenen Epochen ermöglicht.

Insgesamt behandelt diese Dissertation eine umfassende Diskussion des UAV-basierten Laserscannings mit Anwendung in Landwirtschaft und Deformationanalyse. Dabei ergeben sich wertvolle Einblicke für das Verständnis der Punktwolkenqualität und potentielle Ansätze zur Analyse von Daten.

Contents

Preface

This cumulative dissertation presents the investigations of quality aspects in UAV-based laser scanning and its application in agriculture and deformation monitoring. It is based on the following five publications that were all subject to a peer-review process:

- **Publication A** (Peer-reviewed, Journal):
  Dreier, A., Janßen, J., Kuhlmann, H., & Klingbeil, L. (2021a). Quality analysis of direct georeferencing in aspects of absolute accuracy and precision for a UAV-based laser scanning system. *Remote Sensing*, 13(18), 3564, https://doi.org/10.3390/rs13183564
- **Publication B** (Peer-reviewed, Conference):
  Dreier, A., Kuhlmann, H., & Klingbeil, L. (2023a). The potential of UAV-based laser scanning for deformation monitoring - case study on a water dam. *5th Joint International Symposium on Deformation Monitoring (JISDM 2022), Editorial Universitat Politècnica de València*, 2023, 261–269, http://doi.org/10.4995/JISDM2022.2022.13833
- **Publication C** (Peer-reviewed, Journal):
  Dreier, A., Jost, B., Kuhlmann, H., & Klingbeil, L. (2024a). Investigations of the scan characteristics with special focus on multi-target capability for the 2D laser scanner RIEGL miniVUX-2UAV. *Journal of Applied Geodesy*, 18(1), 97–113, https://doi.org/10.1515/jag-2022-0029
- **Publication D** (Peer-reviewed, Journal):
  Dreier, A., Lopez, G., Bajracharya, R., Kuhlmann, H., & Klingbeil, L. (2025a). Structural wheat trait estimation using UAV-based laser scanning data: Analysis of critical aspects and recommendations based on a case study. *Precision Agriculture*, 26(18), https://doi.org/10.1007/s11119-024-10202-4
- **Publication E** (Peer-reviewed, Journal):
  Dreier, A., Tobies, A., Kuhlmann, H., & Klingbeil, L. (2025b). Stone instance segmentation of rubble masonry based on laser scanning point clouds. *Measurement*, 242, 115905, https://doi.org/10.1016/j.measurement.2024.115905

The content of these publications is summarized in Chapter 4, and the most relevant scientific results and contributions are outlined in Chapter 5 of this thesis. The author of this dissertation has made the main contribution to each of these publications and, in particular, has provided the respective methodology.

1. Introduction

The use of laser scanning on Unmanned Aerial Vehicles (UAV) has increased in the last few years due to the rapid development of sensor technology. The concept of UAV-based laser scanning typically utilizes sensors for pose estimation with Global Navigation Satellite System (GNSS) and Inertial Measurement Unit (IMU) as well as a laser scanner [Mandlburger, 2022b]. Algorithms for sensor fusion are used to derive a georeferenced 3D point cloud that is used in applications like mining, topographic and bathymetric surveying, forestry or precision agriculture [Coops et al., 2021; Guan et al., 2016; Guimarães et al., 2020; Mandlburger et al., 2020a; Shahmoradi et al., 2020]. For the entire range of applications where additional parameters or models are derived, the quality of the point cloud is relevant. The error sources within the processing can mainly be separated into uncertainties in trajectory estimation, system calibration, laser scanner errors, and miscellaneous errors [Shan & Toth, 2018]. This dissertation deals with the use of UAV-based laser scanning in the applications of precision agriculture and deformation monitoring. In both areas, the 3D point cloud is used to derive either parameters or models for further analysis. This thesis provides new insights which are valuable for application in practice. Furthermore, the knowledge about the quality of the point clouds captured with UAV-based laser scanning affects the following processing of the data. Therefore, this dissertation also deals with the investigation regarding the quality of the point cloud especially influenced by trajectory estimation and the laser scanner. The main motivation and objectives are described in Sections 1.1 and 1.2.

1.1 Motivation

The use of UAV-based laser scanning benefits from more flexible flight planning and a higher level of detail compared to traditional Airborne Laser Scanning (ALS) [Mandlburger, 2022b]. It provides a faster acquisition of survey objects than static measurements with a Terrestrial Laser Scanner (TLS). Finally, the possibility of direct georeferencing by deriving a 3D point cloud in a global reference frame without external information or ground control points is beneficial for multiple applications. One part of this thesis is the application of UAV-based laser scanning in two different areas: precision agriculture and deformation monitoring. The estimation of structural wheat traits is investigated for the parameters of crop height and Leaf Area Index (LAI), with a discussion of the impact of the laser scanner. Furthermore, the potential of using UAV-based laser scanning in GNSS-denied environments for deformation monitoring is discussed, which revisits the topic of direct georeferencing. In both areas existing approaches or methods are developed further with new methodology or analysis. However, in both areas the 3D point cloud is used for the processing, and knowledge about its quality is necessary, which is a major part of this thesis. The quality analysis and control of the derived point cloud is one of the challenges in static and kinematic laser scanning, which is getting even more complex in the context of multi-sensor systems [Heinz, 2021]. In this case, the point cloud processing includes multiple sensors with uncertainties contributing to the error budget [Habib et al., 2009]. Furthermore, the calibration and synchronization between the sensors becomes relevant. Hence, the understanding of errors contributing to the quality of the point cloud is highly relevant, especially if it is used for subsequent estimation and interpretation of models or parameters in the application. This thesis contributes to the understanding of the error budget in UAV-based laser scanning in terms of direct georeferencing and the laser scanner itself. Since the subjects covered are diverse, the individual motivation for each aspect will be stated in the following.

Direct georeferencing reduces the need for overlapping flight strips and integration of Ground Control Points (GCPs) [Stöcker et al., 2017]. This advantage becomes beneficial in the context of corridor mapping or large areas that have to be covered. Overall, it can lead to time and cost savings in project execution. However, quality assessment of acquired point clouds is always necessary. There are different approaches for evaluating point clouds derived from UAV-based laser scanning or multi-sensor systems in general. Besides the forward modeling of included errors, the evaluation compared to reference parameters or reference point clouds is the most prominent [Heinz, 2021]. Nevertheless, this approach typically assesses the product of a 3D point cloud without the ability to provide the reason for errors traced back to the source, e.g., errors in trajectory estimation or system calibration. The evaluation of the UAV point cloud in comparison to a reference point cloud can be done by point-based, area-based, or parameter-based comparisons [Heinz, 2021]. Furthermore, it can be distinguished between the analysis of precision and accuracy. The precision is often analyzed based on strip comparisons, indicating the quality of the inner geometry of the point cloud [Shan & Toth, 2018]. Furthermore, the repetition of measurement flights can be used in this analysis. The accuracy includes the trueness and, therefore, the analysis of the location and orientation of the point cloud with respect to the global reference frame. Considering this, one impacting factor is the accuracy of the GNSS position included in the processing. Strategies for the evaluation of point clouds from UAV-based laser scanning were already discussed with different emphases [Pilarska et al., 2016; Glennie, 2007; Baltsavias, 1999; Habib et al., 2009; Mandlburger et al., 2020b]. Nevertheless, a detailed investigation focusing on the quality separated in point cloud noise, precision of repeated measurements and accuracy was not shown for this thesis's used sensor system (RIEGL miniVUX-SYS) so far.

As discussed before, the point cloud quality derived from UAV-based laser scanning includes errors from multiple sources. The measurement conditions, which include the flight pattern, weather conditions, and measurement environment, must be considered [Mandlburger, 2022b]. This applies especially to GNSS-denied environments since the quality of direct georeferencing is largely based on GNSS processing. Different approaches have already been developed to improve the point cloud. One important processing step is the strip adjustment, where multiple flight strips covering the same area are used to correct misalignments on the point cloud or trajectory level [Glira, 2018]. Furthermore, the introduction of GCP or reference point clouds is possible. Besides the processing explained, even additional sensors like cameras are integrated within hybrid adjustments [Glira, 2018]. Nevertheless, there is still potential for improvement, especially in challenging GNSS conditions. An environment where these conditions are typically present is data acquisition at water dams with possible limitations in GNSS reception. At the same time, there has already been progress in the recording of such structures with TLS [Alba et al., 2006; Scaioni et al., 2018], which is why aerial surveys with UAVs are also conceivable. However, such an application and the evaluation of the potential has only been done with photogrammetric surveys and an evaluation of UAV-based laser scanning has not been done.

Compared to the quality of the point cloud, including errors from different sources, the quality of the laser scanning sensor can be evaluated individually. This has been shown with a detailed analysis of a 2D profile scanner used in multi-sensor systems in Heinz et al. [2018]. The analysis in this context discusses quality aspects regarding range measurement, such as range precision. Laser scanners in airborne and UAV-based laser scanning are often full-waveform scanners. With the recording of the entire signal reflected, detecting multiple targets (echoes) is possible, referred to as the multi-target capability [Mallet & Bretar, 2009]. This capability provides multiple echoes for a single laser beam emitted by the scanner, which is beneficial, especially in the context of measurements in vegetation, e.g., forestry. Different requirements must be fulfilled to separate the reflected signal of two objects [Ullrich & Pfennigbauer, 2011]. One aspect is the minimum resolvable distance between both objects, which relates to the laser pulse length [Mandlburger, 2022b]. In general, there are already studies investigating different quality aspects of laser scanner theoretically and empirically (e.g. Mandlburger et al. [2020b]; Mallet & Bretar [2009]; Wujanz et al. [2018]), but especially a detailed investigation of the multi-target capability in terms of the minimum distance between targets and the precision of multiple echoes is missing.

One application of UAV-based laser scanning in this thesis is agriculture and the monitoring of plant traits derived from the point cloud. The advantage of laser scanning in this area is similar to that of forestry, where the laser beams can penetrate the crop surface to measure the region below the canopy [Bates et al., 2021]. Depending on the vegetation height, the multi-target capability can be highly beneficial. Monitoring structural plant traits like plant height, leaf area index, or leaf angle distribution can be used for crop health monitoring or breeding applications [Storm et al., 2024]. Challenges in this context are especially the quite small objects like crops in early growing stages in the question of what is measured with the UAV-based laser scanning system. Considering the resolution capability of the sensor, it is not always possible to resolve objects to a high level of detail. Furthermore, the spatial resolution is important to guarantee the completeness of captured objects. There are already studies investigating the derivation of crop heights and LAI from point clouds in general (e.g. Bates et al. [2021]; Lei et al. [2019]). Nevertheless, a detailed analysis of the impacting factors in this processing is missing so far. This relates especially to the impact of soil filtering in the pre-processing step and the impact of the extinction coefficient within the LAI estimation.

1.2 Objectives

This thesis investigates different quality aspects and the application of UAV-based laser scanning in precision agriculture and deformation monitoring. The objectives (1.) and (2.) focus on the strategies for evaluating a UAV-based laser scanning system without specification of the intended application. This is followed by the application in agriculture in objective (3.) with the derivation of structural plant traits. The last objective (4.) deals with the application in deformation monitoring with the quality analysis of derived point cloud and an approach for stone instance segmentation. The five Publications A - E contributing to this thesis are included in the following description separated into four main objectives:

1. **Evaluation of direct georeferencing using UAV-based laser scanning** - Since especially direct georeferencing in UAV-based laser scanning systems provides multiple benefits, strategies for analyzing the quality of the 3D point clouds are presented. The approach focuses on four aspects: point cloud noise, accuracy, precision of repeated measurements, and the impact of the GNSS master station used. The investigations include two typical flight patterns in UAV-based laser scanning with cross-flight and corridor mapping (Publication A [Dreier et al., 2021a]).
2. **Investigations of quality aspects of a full-waveform 2D laser scanner** - The laser scanner itself impacts the error budget of UAV-based laser scanning. Therefore, strategies for evaluation focusing on the quality assessment of a 2D laser scanner (RIEGL miniVUX-2UAV) within a multi-sensor system, excluding pose estimation sensors, are presented. Key parameters evaluated include range precision, rangefinder offset, resolution capability, and multi-target capability (Publication C [Dreier et al., 2024a]).
3. **Estimation of structural plant traits with plant height and leaf area index** - The estimation and analysis of structural wheat traits, specifically crop height and leaf area index, using a UAV-based laser scanning system is analyzed. Besides the parameter estimation, it introduces a novel ground classification algorithm that separates ground points from crop points using k-means clustering based on geometric and radiometric features. The quality of estimated traits is investigated in terms of the resulting accuracy and the aspects of soil filtering and the impact of the extinction coefficient in LAI estimation (Publication D [Dreier et al., 2025a]).
4. **Analysis of UAV-based laser scanning for deformation monitoring of a water dam** - The potential of UAV-based laser scanning for monitoring a water dam is investigated. This addresses difficulties in trajectory estimation, flight planning, and the unique measurement environment. This new investigation highlights the potential but also limitations under difficult GNSS conditions (Publication B [Dreier et al., 2023a]). After point cloud generation, the analysis of deformations requires algorithms to compare two point clouds. The development of an instance segmentation algorithm for rubble masonry is presented to enhance this goal (Publication E [Dreier et al., 2025b]).

This thesis is structured as follows. The scientific context is given in Chapter 2 followed by the theoretical basics in Chapter 3. The publications contributing to this thesis are summarized in Chapter 4 and the most important aspects are given in Chapter 5 in more detail. This is followed by considerations for future research in Chapter 6 and summarized in the conclusion in Chapter 7.

2. Scientific context

With the development of sensor technology, the concept of kinematic laser scanning available in airborne laser scanning (ALS) was transferred to the use of UAVs. Since the measurement and processing concepts are very similar, the quality assessment and assurance methods can be used for ALS and UAV-based laser scanning. This thesis deals with the quality analysis of different aspects of UAV-based laser scanning and two applications, for which the scientific background is given in the following. The corresponding research questions are according to the four objectives of this thesis and are raised within this part.

The evaluation of UAV-based laser scanning can typically be divided into theoretical and empirical studies. A theoretical approach is described by Pilarska et al. [2016], which focuses on the propagation of errors in the position and orientation of the UAV to the point cloud. In addition, Glennie [2007] also considers the errors introduced by the calibration of the system with boresight angles and lever arm. Further studies on the error budget for airborne or UAV-based laser scanning systems are Baltsavias [1999]; Shan & Toth [2018]; Habib et al. [2009]. The critical aspect of the theoretical approaches is the consideration of all errors. For this reason, most quality assessments to date have been carried out on the basis of the empirical approaches. Examples for the empirical investigation of point cloud quality can be found in Tulldahl et al. [2015] or studies with additional optimization strategies in Mandlburger et al. [2020a].

Different approaches are recommended for the empirical evaluation of point clouds, which can be divided into (1) point-based, (2) area-based, and (3) parameter-based strategies [Heinz, 2021]. The evaluation is made in comparison to a higher-order reference. These reference points or point clouds are determined by traditional surveying methods such as total stations, GNSS, leveling or TLS. Typical objects for point-based evaluation can be natural objects (e.g. building corners, road markings or manholes) or artificial objects (e.g. targets or checkerboard patterns) [Hesse, 2008; Lim et al., 2013; Kukko et al., 2012; Barber et al., 2008; Kaartinen et al., 2012; Schlichting et al., 2014]. One challenge with point-based evaluation methods and UAV-based laser scanning lies in the comparatively low point density with increasing flight altitude and speed, which must be taken into account during flight planning. In addition to the point-based evaluation, the area-based strategies are often used for comparison with a known reference point cloud (e.g. TLS) [Kaartinen et al., 2012; Toschi et al., 2015; Gräfe, 2009; Tucci et al., 2018]. For the calculation of the differences, various algorithms such as the cloud-to-cloud distance or the Multiscale Model to Model Cloud comparison (M3C2) method are used [Lague et al., 2013]. The third possibility of the above-mentioned evaluation strategies is the parameter-based evaluation [Kaartinen et al., 2012]. Potential parameters are typically derived from objects with a defined geometric shape. Furthermore, several studies investigated the quality for the calculation of forest structure properties (e.g. stem diameter, volume) in forestry [Brede et al., 2017; Dalla Corte et al., 2020; Cao et al., 2019]. Similar to the previous evaluation methods, parameter-based evaluation can also be used to analyze accuracy.

The quality of point clouds generated by multi-sensor systems has been the subject of multiple studies. While previous studies have focused on evaluating the overall system's performance, few have delved into how individual factors, such as the laser scanner itself, contribute to error budget. Studies like Wujanz et al. [2018]; Schmitz et al. [2019]; Winiwarter et al. [2020] have developed stochastic models to assess range precision based on signal amplitude, and Heinz et al. [2018] proposed a simplified approach for 2D scanners. Calibration parameters, such as range finder offsets, are crucial for ensuring accuracy, as highlighted in Medić [2021] or Martin & Gatta [2006]. Resolution capability, defined as the ability to distinguish between two objects, has also been extensively studied, especially for 3D laser scanners [Boehler et al., 2003; Huxhagen et al., 2011; Schmitz et al., 2020]. However, investigating resolution capability in systems that integrate multiple sensors, like UAV-based laser scanning, is more complex and time-consuming due to additional variables like scanning parameters or flight parameters [Mandlburger et al., 2020a]. Furthermore, the capability of full-waveform scanners to capture multiple targets has been explored, with significant attention given to improving peak detection within waveforms [Mallet & Bretar, 2009]. Nevertheless, there are no studies in which the precision of two echoes extracted from the full-waveform has been investigated.

An important component of smart farming and also breeding experiments is the monitoring of crops in the form of phenotyping. These are parameters that provide quantitative information about the condition of the crops. Potential parameters derived with UAV-based laser scanning are the crop height and Leaf Area Index (LAI). Crop height, defined as the distance from the ground to the top of the crop, is a critical parameter for understanding crop development and how plants respond to various stress factors like water or nutrient deficiencies [Perez-Harguindeguy et al., 2016]. The approach relies on the Canopy Height Model (CHM) derived from the point cloud generated during a single UAV flight [Becirevic et al., 2019]. However, the precision of these estimates is influenced by several factors, including soil filtering and sensor specifications. A crucial aspect is the interaction between the laser beam and the plant surface, which significantly affects the measurement results [Dreier et al., 2024a]. The LAI, a unitless measure of leaf area per unit of ground surface, is widely used in agriculture to model mass and energy exchanges between the biosphere and atmosphere [Yan et al., 2019; Krinner et al., 2005]. While various definitions of LAI exist, the Plant Area Index (PAI) is often used in the context of UAV-based laser scanning to compute the relationship between plant area and ground area [Fang et al., 2019]. Multiple studies have explored deriving the LAI parameter from images or laser scanning data [Roth et al., 2018; Bates et al., 2021; Solberg et al., 2006], with laser scanning offering significant advantages due to its independence from lighting conditions and its ability to penetrate the crop canopy [Lei et al., 2019]. Algorithms that process point clouds to derive LAI depend on several assumptions or generalizations, such as the presumed leaf angle distribution [Solberg et al., 2006]. One possibility is the gap-based approach, based on the Beer-Lambert law, which correlates the amount of light absorbed within the crop canopy to the LAI [Wang & Fang, 2020]. However, this approach depends on two critical factors: the accurate separation of soil and crop points, and the correct choice of extinction coefficient in the PAI calculation. These factors are the primary focus of this thesis, as they represent the main limitations and potential areas for improvement in LAI estimation using UAV-based laser scanning.

UAV-based laser scanning has been used in various applications, especially for monitoring large, challenging-to-reach areas such as landslides, glaciers, land deformations, and forestry. Recent studies have begun to discuss the use of UAV-based laser scanning for deformation analysis. For instance, it has been applied to monitor landslides by estimating and comparing roof areas across different time periods [Zieher et al., 2019]. It has also been used to detect land deformations, such as those caused by mining activities, often in combination with TLS and UAV photogrammetry to detect deformations in the range of several decimeters [Jóźków et al., 2021]. In the studies so far, these deformations are identified by generating Digital Elevation Models (DEMs) from data collected at different times, then evaluating them with results from TLS or total stations [Moudrỳ et al., 2019; Wang et al., 2020; Zhang et al., 2016]. UAV-based laser scanning is mostly employed for detecting deformations with magnitudes in the centimeter to decimeter range, which may not meet the higher accuracy demands required for dam monitoring. Although TLS is a well-established method for dam monitoring, offering precise analysis based on point clouds [Alba et al., 2006; Scaioni et al., 2018; Xu et al., 2018], adapting similar methods to UAVs has been limited due to the accuracy. This thesis investigates the potential of UAVs for dam monitoring, leveraging their advantages while addressing the challenges posed by the requirements. Based on the captured point cloud, algorithms for epoch comparison are necessary to evaluate potential deformation. These approaches would be highly beneficial if identical objects, e.g., stones are detected in a pre-processing step. Approaches for stone segmentation vary depending on whether they are applied to point clouds or images. Image-based methods, for example, use semi-automatic algorithms for delineating stone masonry [Yang et al., 2023]. However, these methods depend on color information, which is not always available in laser scanning data. Consequently, point cloud-based algorithms are necessary for certain applications, particularly in cultural heritage contexts. For example, techniques like instance segmentation using random forest classification and density-based clustering have shown promising results for segmenting grains in riverbeds [Galanakis et al., 2023; Chen et al., 2016]. Since some methods rely on geometric features for segmentation, such approaches may not be sufficient for structures like rubble stone masonry, where there is no clear separation based on joint depth or shape. For example, tools developed for stone wall segmentation on TLS point clouds have proven to be effective when the geometry allows for a clear separation between stones and joints [Wiedemann & Holst, 2023]. However, in the case of dams, where such clear separations are often lacking, new approaches are needed. This thesis includes a novel method for instance segmentation based solely on point cloud data, utilizing 3D point information and the intensity attribute, which describes the reflected signal intensity.

3. Theoretical basics

UAV-based laser scanning is a method for capturing the 3D environment using a UAV equipped with a lightweight laser scanner. Compared to ALS, it enables lower flight altitudes and velocities, resulting in more details in the 3D point cloud when acquiring objects like infrastructure or vegetation [Mandlburger, 2022b]. One example of a point cloud coming from UAV-based laser scanning is shown in Figure 3.1 with the point cloud including RGB colorization (left) and intensity colorization (right). This section provides the theoretical basis for the scientific contributions of this work, which are necessary for the processing of a point cloud, focusing on the principle of UAV-based laser scanning.

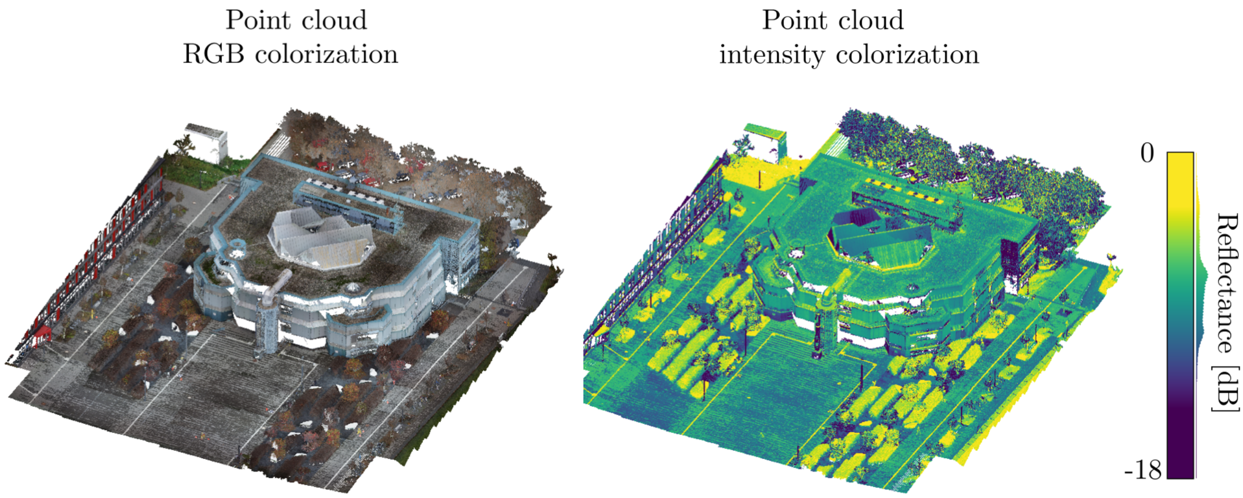

Figure 3.1: Point cloud captured with a UAV-based laser scanning with RGB colorization (left) and intensity colorization (right).

Therefore, the fundamental concept of LiDAR (Light Detection And Ranging) is explained in Section 3.1 with a special focus on the multi-target capability of full-waveform laser scanners. Besides the part of the laser scanner itself, system calibration and trajectory estimation are important for calculating 3D point clouds in a global coordinate system (e.g., ETRS89). With direct georeferencing, the parts of trajectory, system calibration, and laser scanner measurements are finally combined into the point cloud. Typically, even further improvement of the result is performed by the introduction of ground control points or the improvement of the entire trajectory by strip adjustment. The concept of direct georeferencing with the corresponding error budget, system calibration, and strip adjustment is summarized in Section 3.2 in the context of UAV-based laser scanning. Finally, the sensor system used throughout this work is presented shortly in Section 3.3 with the most important specifications.

3.1 LiDAR basics

In this section, the basics of LiDAR (Light Detection and Ranging) are given, which are generally similar for use in ALS and UAV-based laser scanning. This part is separated into Section 3.1.1 with an explanation of the rangefinder and scanning concept. Further, Section 3.1.2 discusses the concept of multi-target capability in more detail.

3.1.1 Laser ranging and scanning

The rangefinder unit in a laser scanner measures the distance to a reflective object such as ground, buildings, or vegetation. In general, there are two prominent technologies: (1) the time of flight (TOF) method and (2) the phase shift method [Mandlburger, 2022b]. Since most of the scanners used in the context of ALS and UAV-based laser scanning are time of flight measuring systems, the following part only describes this method. If not mentioned specifically, the following information can be found in Shan & Toth [2018]. Based on the known speed of light c, the laser pulse emission time t_s, laser pulse arrival time t_i, the distance between target and sensor R_i is calculated with

$$R_i = \frac{1}{2}\left(t_i - t_s\right) c \quad . \tag{3.1}$$

Considering that the speed of light is correct and the beam hits one planar surface, the accuracy of the range measurement is dependent on the timing accuracy [Mandlburger, 2022b]. Besides this, several other factors influence the signal power received by the rangefinder. The relationship between emitted and received optical power is described by the laser-radar equation as

$$P_E = \frac{P_S D_E^2}{4\pi\gamma_s^2 R^4} \cdot \sigma \cdot \eta_{ATM} \cdot \eta_{SYS} \quad . \tag{3.2}$$

The received power P_E depends on the transmitted power P_S, the size of the receiver's aperture D_E, the beam opening angle γ_s, the measurement range R, backscatter cross-section σ, the atmospheric loss η_{ATM} and the system loss η_{SYS}. The backscatter cross-section σ summarizes the impact due to the object properties and can be further described with

$$\sigma = \frac{4\pi A\rho}{\Omega} \tag{3.3}$$

including the target area A, the reflectance of the object ρ, and the backscattering solid angle Ω. The last angle describes the geometry of the cone into which the laser beam is reflected back to the sensor. This depends on the object and is typically separated into specular reflection, diffuse reflection, or the special case of isotropic reflection.

One important aspect of the cross-section is the illuminated target area A, which depends again on multiple factors. Depending on the object size, it relates to the footprint size and can be calculated by

$$A = \frac{A_L}{\cos\alpha} \approx \frac{\gamma_s^2 R^2 \pi}{4\cos\alpha} \quad . \tag{3.4}$$

The area A_L is the projection of the illuminated area to the orthogonal plane relative to the laser beam direction. This part depends on the beam opening angle γ_s and the measurement range R. Furthermore, the incidence angle α between the laser beam and the surface's normal is considered.

In addition to the rangefinder unit itself, the area-based measurement of laser sensors is achieved by using a rotating beam deflection in different scanning patterns and the movement of the entire platform in the region of interest. The most prominent variations of beam deflection are shown in Figure 3.2 with (a) a rotating polygon, (b) a rotating wedge, (c) a Palmer scanner, and (d) an oscillating mirror, which differ from the most in the resulting scan pattern [Mandlburger, 2022b]. The (a) rotating polygon rotates at a constant speed, resulting in constant point spacings within each scan line. Depending on the rotation speed, the pulse repetition rate (PRR), and the UAV flight speed, the point spacing on the ground can be constant in flight direction. The (b) rotating wedge is constructed with a 45° tilted mirror rotating around the horizontal axis. This configuration enables the scan of a 360° profile, which is often obstructed due to the UAV. Depending on the same configuration as before, the scan pattern on the ground can have a constant spacing. Nevertheless, due to the scan geometry, the point spacing increases with increasing distance from the nadir direction. The

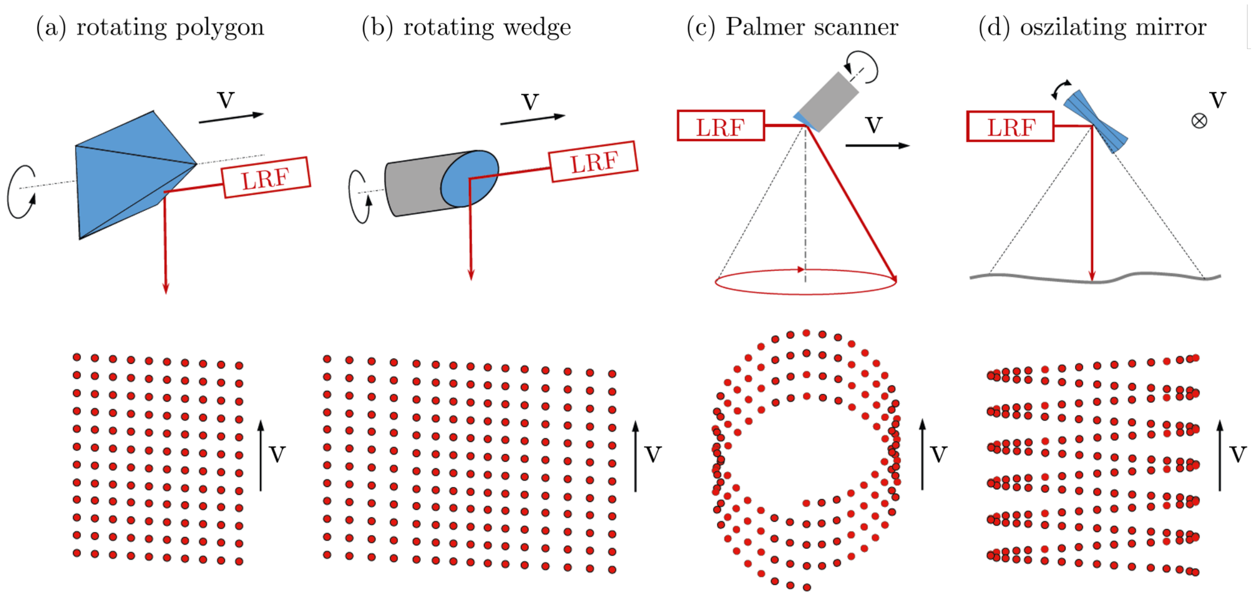

Figure 3.2: Mechanical scanning variations for UAV-based laser scanning (adapted from [Mandlburger, 2022a]).

frequently used (c) Palmer scanner uses a constant off-nadir angle of the laser beam. This configuration results in a spiral-shaped pattern on the ground. Due to the constant tilt of the scan, it is better to capture vertical structures like buildings or even use them in bathymetry, where an off-nadir angle is necessary to penetrate the water. Compared to the previous types, the Palmer scanner measurements result in an inhomogeneous pattern on the ground with higher point density at the border of the flight line. The (d) oscillating mirror performs a small movement of the mirror between two positions, resulting in an oscillating pattern on the ground. Similar to the Palmer scanner, point densities are higher at the border of the flight line. The presented scanning types have different advantages and disadvantages, as well as different areas of application. The used scanner type in this work is only the rotating wedge. Besides the mentioned variations, there are also a large amount of multi-beam LiDAR scanners [Mandlburger, 2022b], which are not further discussed in this work.

3.1.2 Multi-target capability

The multi-target capability of laser scanners is based on full-waveform processing, which is done online or in post-processing [Ullrich & Pfennigbauer, 2011]. The general concept is shown in Figure 3.3 with the reflected laser signal recorded over time with corresponding amplitude. Having the full-waveform of the reflected signal, different algorithms can be used to detect peaks within the waveform and the corresponding time, respectively, range measurement [Mallet & Bretar, 2009]. Therefore, one single laser beam can be used to detect different objects, e.g., branches, leaves, or the ground. The limitation of detecting subsequent echoes is imposed by the sensor specification and the pulse length T_P. The minimum resolvable distance between two targets ΔR_{tar} is derived by

$$\Delta R_{tar} = \frac{c}{2} T_P \tag{3.5}$$

including the speed of light c [Shan & Toth, 2018; Mandlburger, 2022a]. Typical pulse lengths in ALS or UAV-based laser scanning are about 1 ns - 10 ns, leading to a minimum resolvable distance of 15 cm - 1.5 m.

Besides detecting individual echoes, additional attributes are typically derived using the full-waveform within the signal processing [Ullrich & Pfennigbauer, 2011]. However, these attributes are also dependent on the

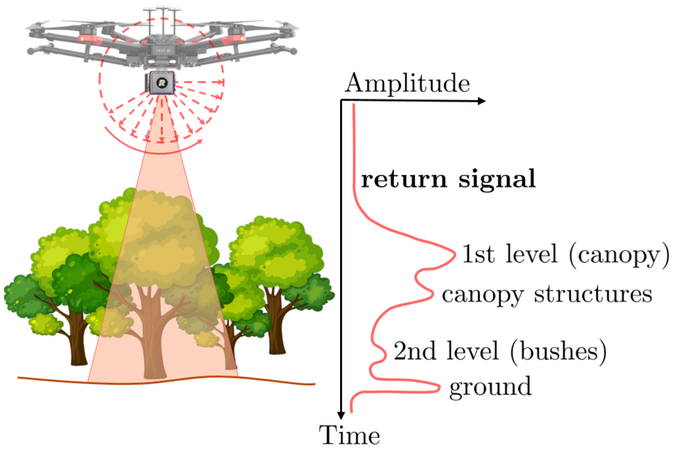

Figure 3.3: Multi-target capability based on full waveform processing.

sensor and, therefore, the manufacturer. The amplitude describes the optical power of the target's echo signal. Since this attribute is typically highly dependent on the target distance, the attribute reflectance is also given. The reflectance is the ratio of the target's echo signal power to the echo signal power returned from a white target at the same distance. Furthermore, the echo width or pulse shape deviation is provided. This deviation indicates the difference between the echo pulse shape and the pulse shape received from a flat target at a perpendicular angle of incidence [Pfennigbauer & Ullrich, 2010]. The deviation can be interpreted as a measure of the trustworthiness of a point and thus relates to the quality of measurement.

3.2 UAV-based laser scanning

This section explains the general concept of UAV-based laser scanning, starting with raw sensor data up to the creation of the point cloud. Besides the principle of direct georeferencing, the error budget is also explained in Section 3.2.1. Afterward, the improvement of the point cloud based on overlapping flight strips is discussed in Section 3.2.2, followed by a short overview of flight planning in Section 3.2.3.

3.2.1 Direct georeferencing and error budget

The concept of direct georeferencing in UAV-based laser scanning is always based on sensors to localize the UAV with positions and orientations over time, as well as the laser scanner and an optional camera [Glira, 2018]. The entire processing, starting with the raw data (blue boxes) and ending with the 3D point cloud (green box), is shown in Figure 3.4 with additional processing steps (orange boxes). A combination of GNSS and IMU measurements is typically used for trajectory estimation with the platform's positions and orientations. The GNSS observations are usually processed in differential mode with the observations from an additional GNSS master station and then fused with the IMU data using a Kalman filter or similar algorithm, resulting in the trajectory [Pöppl et al., 2023]. With subsequent georeferencing of time-synchronized laser scans based on the trajectory and laser scanner measurements, the georeferenced 3D point cloud is created (as shown in Figure 3.1). Additional information needed in this processing chain is the system calibration parameters describing the relative positions and orientations between the sensors on the platform. The three types of data with trajectory, calibration parameters, and laser scanner measurement can be combined by

$$\mathbf{x}^e_{[t]}(t) = \mathbf{g}^e(t) + R^e_n(t) R^n_i(t) \left(\mathbf{a}^i + R^i_s \mathbf{x}^s_{[t]}\right) \tag{3.6}$$

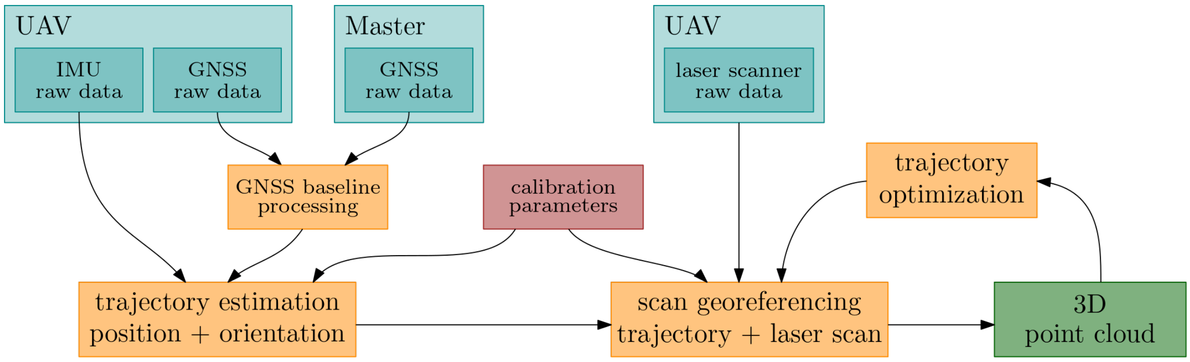

Figure 3.4: Processing of UAV-based laser scanning data, including trajectory estimation and scan georeferencing.

resulting in the 3D coordinates $\mathbf{x}^e$ of object point $[t]$ in a global coordinate system at time t. The used notation is based on Glira [2018]. The vector $\mathbf{x}^s$ describes the scanner measurement in the scanner coordinate system (s-system). Furthermore, transformations R between the IMU coordinate system (i-system), navigation system (n-system), and Earth-Centered, Earth Fixed (ECEF) coordinate system (e-system) are included. The vector $\mathbf{g}^e$ describes the position in the ECEF system based on GNSS as part of the trajectory data. The system calibration is included with the lever arm $\mathbf{a}^i$ with $(\Delta a^i_x, \Delta a^i_y, \Delta a^i_z)$ and the rotation R^i_s with Euler angles $(\Delta\omega, \Delta\varphi, \Delta\kappa)$ correcting the boresight misalignment. The included parameters are visualized in Figure 3.5 with the corresponding effect of the individual error. Next to these calibration parameters, sometimes calibration parameters of the laser scanner are included with bias and scale parameters (depending on scanner type) [Glira, 2018]. Based on the necessary data and explained processing, the georeferenced 3D

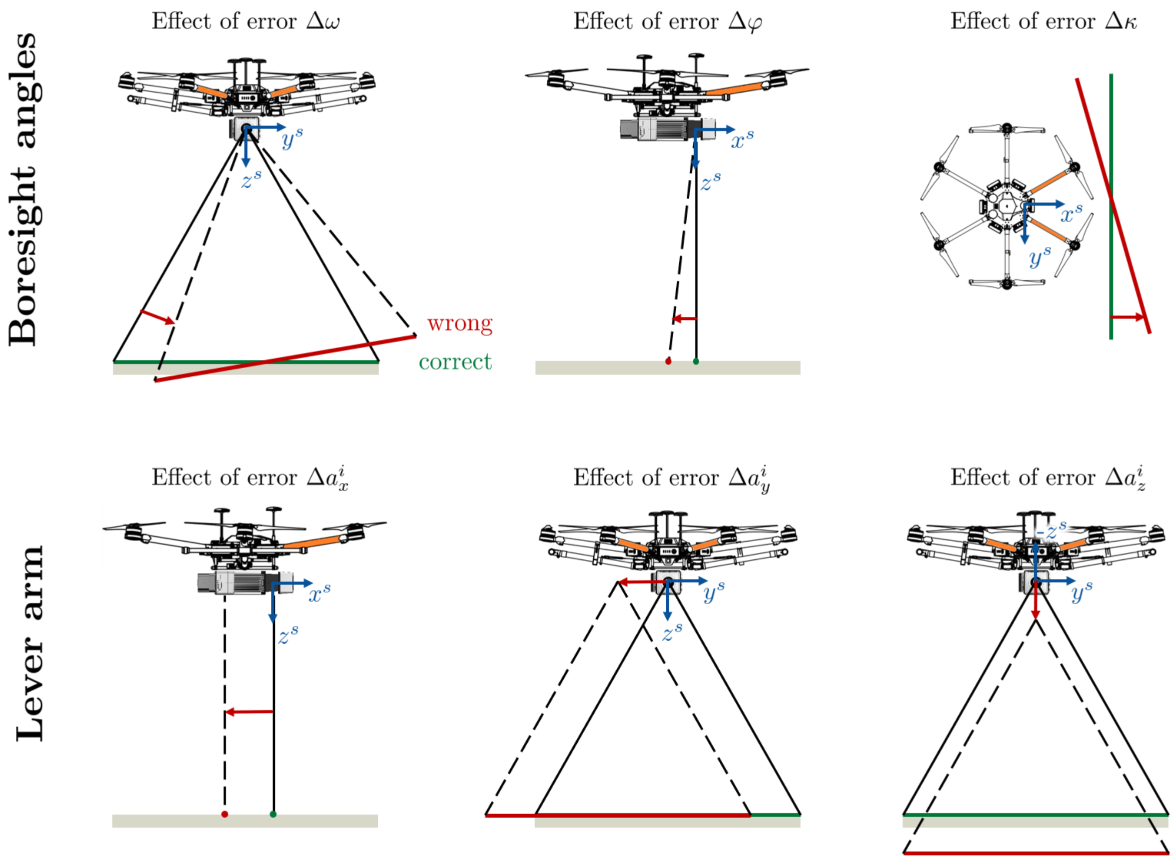

Figure 3.5: Calibration parameters and effect of errors in UAV-based laser scanning system separated in boresight angles and lever arm (adapted from Glira [2018]).

point cloud can be calculated. Since uncertainties are included in the processing, a typical correction step is performed by the strip adjustment using overlapping flight strips, which is explained in the next section. More details regarding the functional model of direct georeferencing can be found in Glira [2018].

The uncertainty of the point cloud is a combination of several systematic and random errors that affect the estimation process [Shan & Toth, 2018], summarized in Table 3.1. Most of the errors in Table 3.1 can be

Table 3.1: Major error sources for UAV-based laser scanning systems (refer to Shan & Toth [2018]).

	Errors
Trajectory estimation	Errors in position and orientation-sensor platform
System calibration	error in lever arm (GNSS antenna and IMU) error in lever arm (laser scanner and IMU) bore-sight angle error between IMU body and laser scanner
Laser scanner	range measurement error object characteristics atmospheric refraction
Miscellaneous errors	time synchronization sensor mounting rigidity

assigned to the parameters contained in the direct georeferencing equation. Typically, the most significant errors that occur in UAV-based laser scanning are included in the GNSS/IMU-based trajectory estimation, which can be expressed as platform position and orientation errors. Further errors are associated with the calibration of the system with the lever arms and correction angles described above. These errors also systematically affect the point cloud quality. In addition, laser scanner measurements may contain errors due to atmospheric refraction, object characteristics, and the error of the distance and angle measurement itself. The miscellaneous errors are due to the timing and stiffness of the sensor support.

3.2.2 Strip adjustment

The measurement flight in UAV-based laser scanning is typically performed with overlapping areas in consecutive flight strips, which are used to improve the point cloud and reduce misalignments [Glira, 2018].

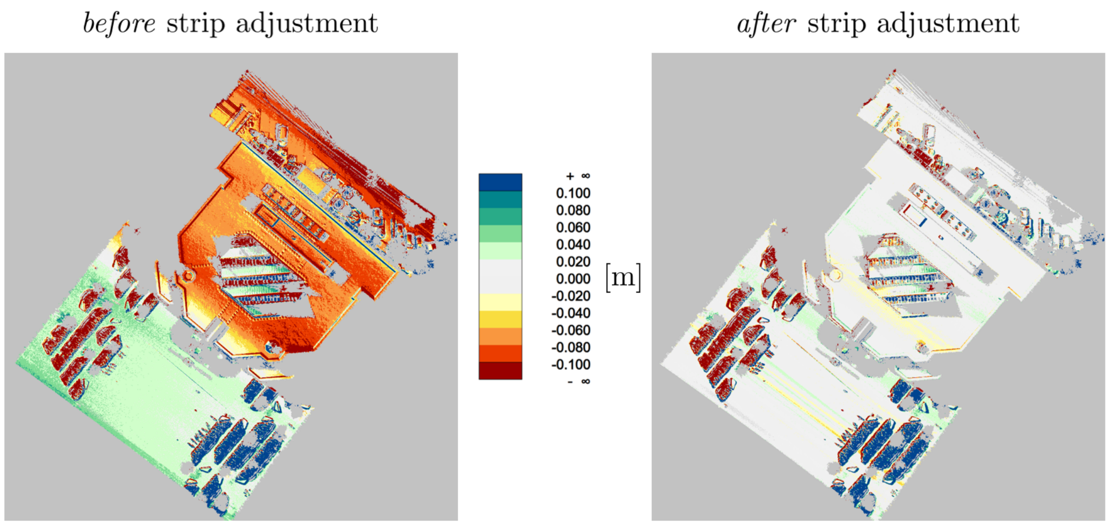

Figure 3.6: Differences between two UAV flight strips *before* and *after* the strip adjustment.

This approach of strip adjustment is shown in Figure 3.6 based on the differences between two flight strips *before* and *after* the performed adjustment. The left part shows the difference between the point clouds after direct georeferencing and the included time-dependent errors of the estimated trajectory (e.g., due to satellite constellation or flight maneuvers). These discrepancies are reduced substantially after the strip adjustment using the OPALS software [Pfeifer et al., 2014]. This adjustment performs a correction of the trajectory based on the minimization of, e.g., point-to-plane distances between the different flight strips. The estimated parameters are corrections to the UAV positions and orientations over time. The complexity of the correction model can be simple with bias parameters for each flight strip up to more complex models with spline corrections for a given time interval. Besides correcting the trajectory, calibration parameters with lever arm and boresight angles can be estimated. Next to the correction model, the algorithm for strip adjustment typically includes steps for finding overlapping areas, subsampling, and finding correspondences solved in an iterated adjustment. Further details about the approach also used within this thesis can be found in Glira [2018].

3.2.3 Flight planning

The flight planning in UAV-based laser scanning is typically performed in consecutive flight strips, where different flight parameters must be defined. Besides adjacent flight strips, cross strips are often used to increase block stabilization and coverage, e.g., in urban areas [Mandlburger, 2022b]. Figure 3.7 shows most of the flight parameters for a 2D profile scanner. The left part shows the chosen field of view Θ (typically up to 90°) and the corresponding maximum range R_{max} [Shan & Toth, 2018]. Based on these parameters

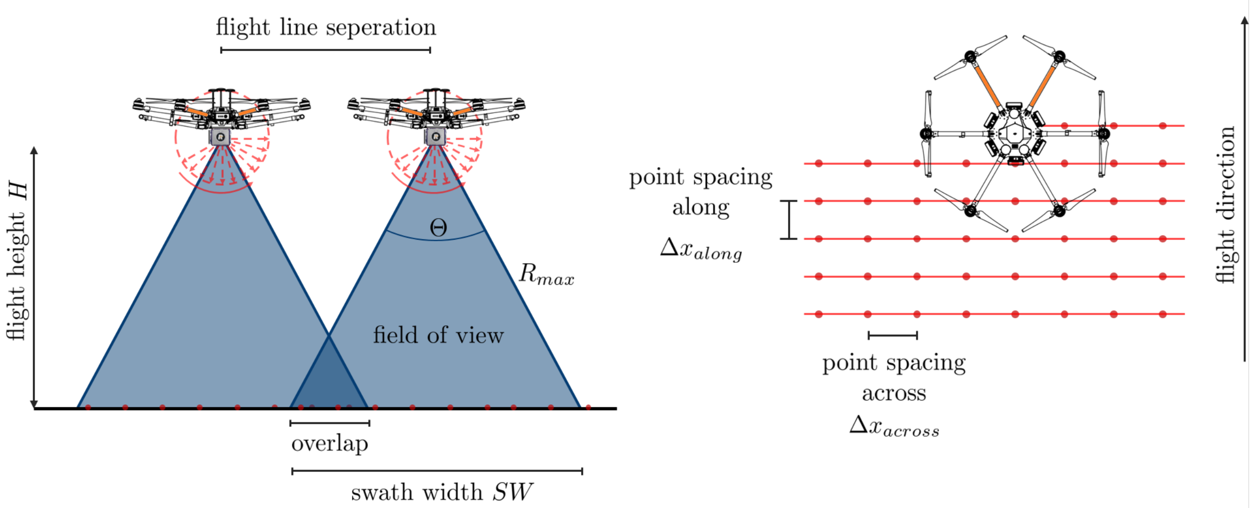

Figure 3.7: Most important parameters necessary for flight planning in case of a 2D profile scanner.

the flight height H and the swath width SW are calculated with

$$H = R_{max} \cdot \cos\left(\frac{\Theta}{2}\right) \qquad \text{and} \qquad SW = 2 \cdot H \cdot \tan\left(\frac{\Theta}{2}\right) \quad . \tag{3.7}$$

This configuration further shows the overlap of adjacent flight strips (typically 20% - 50%). With the defined flight speed v, the flight parameters are defined, and only the laser scanner configuration is left. Together, the parameters of point spacing along Δx_{along} and across Δx_{across} the flight direction are calculated with

$$\Delta x_{across} = \frac{\Theta}{N} \cdot \frac{H}{\cos^2\left(\frac{\Theta}{2}\right)} \quad \text{and} \quad \Delta x_{along} = \frac{v}{f_{sc}} \quad . \tag{3.8}$$

For the point spacing along flight direction, the flight speed and scan speed f_{sc} are necessary. For the point spacing across flight direction, the points per scan line N are included depending on scan frequency and speed. Furthermore, the point density PD can be derived by

$$PD = \frac{MR}{SW \cdot v} \tag{3.9}$$

describing the fraction of points per second divided by area per second. The measurement rate MR is typically smaller than the laser pulse repetition rate PRR in the case of a 2D profile scanner. Next to this, the overlapping factor ξ and the line separation e are calculated by

$$\xi = 1 - \frac{e}{SW} \quad \text{and} \quad e = SW \cdot (1 - \xi) \quad . \tag{3.10}$$

The flight parameters depend highly on the application and the aim of point cloud acquisition. Nevertheless, the parameters are often set based on the spatial resolution and point density of the point cloud. For the case of a 2D profile scanner, the parameters can be chosen so that the point spacing along and across flight direction is equal. The calculation of the point spacing is different for other scanners like Palmer scanners and is based only on single flight strips in this calculation.

3.3 Specifications of the UAV-based sensor system

The theoretical basics of UAV-based laser scanning provide the background for the following publications contributing to this thesis. Since all the studies use the same UAV-based laser scanning system, which is crucial for evaluating the results, it is explained in this section. The UAV-based laser scanning system is shown in Figure 3.8 with the most important components. It is based on the DJI Matrice 600 Pro platform

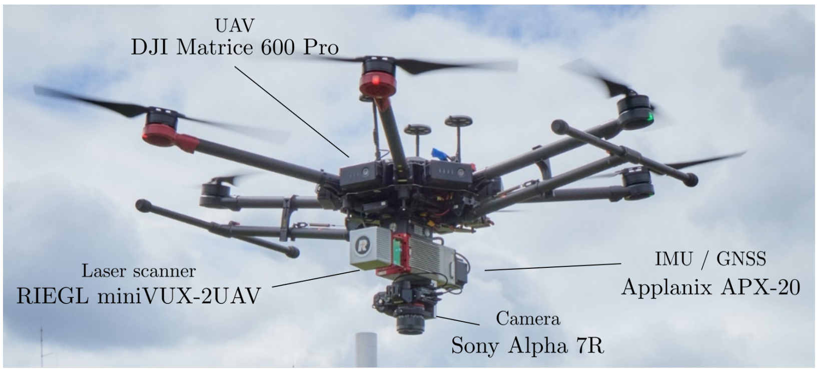

Figure 3.8: UAV-based laser scanning system used for the studies within this thesis based on the DJI Matrice 600 and a RIEGL miniVUX-SYS.

and the lightweight RIEGL miniVUX-SYS, which is designed for use with a UAV. The miniVUX-SYS is a combination of the full-waveform 2D laser scanner RIEGL miniVUX-2UAV and the IMU/GNSS Applanix APX-20 UAV for trajectory estimation. The measurement and processing with this system follow the concept of direct georeferencing explained in Section 3.2.1. Besides the raw data recorded by the laser scanner and IMU/GNSS sensor, one additional master GNSS station is used for processing, whether it is its own station or a virtual reference station.

The scanner is shown in Figure 3.9 with an additional table of specifications. The design is based on a rotating mirror resulting in a 360° profile. The scan speed of the mirror can be set between 10 - 100 lines per second (lps) and the laser pulse repetition rate (PRR) of 100 kHz or 200 kHz. Furthermore, the range

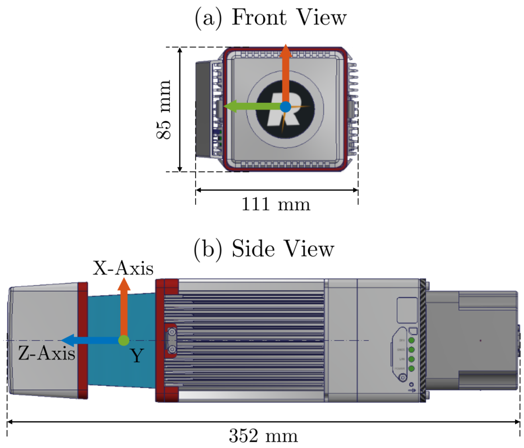

Specifications	
Measuring Principle	time of flight, online waveform processing
Minimum Range	2 m
Accuracy (1σ @ 50 m)	15 mm
Precision (1σ @ 50 m)	10 mm
Max. Number of Targets per Pulse	5
Laser Pulse Repetition Rate (PRR)	100 kHz / 200 kHz
Scan Speed	10 - 100 lps (lines per second)
Laser Wavelength	905 nm (near infrared)
Laser Beam Divergence (FWHM)	1.6 x 0.5 mrad
Laser Beam Footprint	160 mm x 50 mm @ 100 m
Field of View	up to 360°
Angular Step Width $\Delta\varphi$	$0.018° \leq \Delta\varphi \leq 0.36°$
Angle Measurement Resolution	0.001°

Figure 3.9: Specifications and dimensions of RIEGL miniVUX-2UAV (includes Applanix APX-20).

measurement is specified with an accuracy of 15 mm and precision of 10 mm (1σ @ 50 m). Another important aspect is the measurement principle, which is based on the concept of time of flight and online waveform processing. This also provides the multi-target capability and the detection of five target echoes per laser shot as explained in Section 3.1.2. For the investigation of the laser scanner in one of the publications, the laser beam divergence of 1.6 x 0.5 mrad is important (specified as full width at half maximum (FWHM)). Additional attributes are provided for each point in addition to the range measurement. The most important ones, which are used in different applications, are the signal's amplitude, the pulse shape deviation, and the echo number.

Given the quality of the point cloud, which was calculated based on direct georeferencing, the trajectory must be considered. Based on the manufacturer's specification, the trajectory's accuracy is given in Table 3.2 for the UAV pose. The accuracy of positions is given with <0.10 m in vertical and <0.05 m in horizontal

Table 3.2: Error budget of the UAV-based laser scanning system based on RIEGL miniVUX-SYS with APX-20 according to manufacturer's specification [RIEGL Laser Measurement Systems GmbH, 2020, 2021].

Accuracy	Values
trajectory estimation-position vertical	<0.10 [m]
trajectory estimation-position horizontal	<0.05 [m]
trajectory estimation-roll & pitch	0.015 [deg]
trajectory estimation-heading	0.035 [deg]
laser scanner	0.015 [m]

direction. The orientations are given with 0.015° in roll and pitch direction and 0.035° for the heading. Based on these, it is apparent that the accuracy of the trajectory of this UAV-based laser scanning is a major influencing factor. Nevertheless, the specifications so far are given without additional trajectory improvements, which can be achieved, e.g., by strip adjustment or introduction of GCPs.

4. Content of the relevant publications

The content of relevant publications contributing to this thesis is shown in Figure 4.1 with Publications A - E. It is separated into three major topics: the analysis of quality aspects of UAV-based laser scanning and the two applications, precision agriculture and deformation analysis. The quality analysis of direct georeferencing

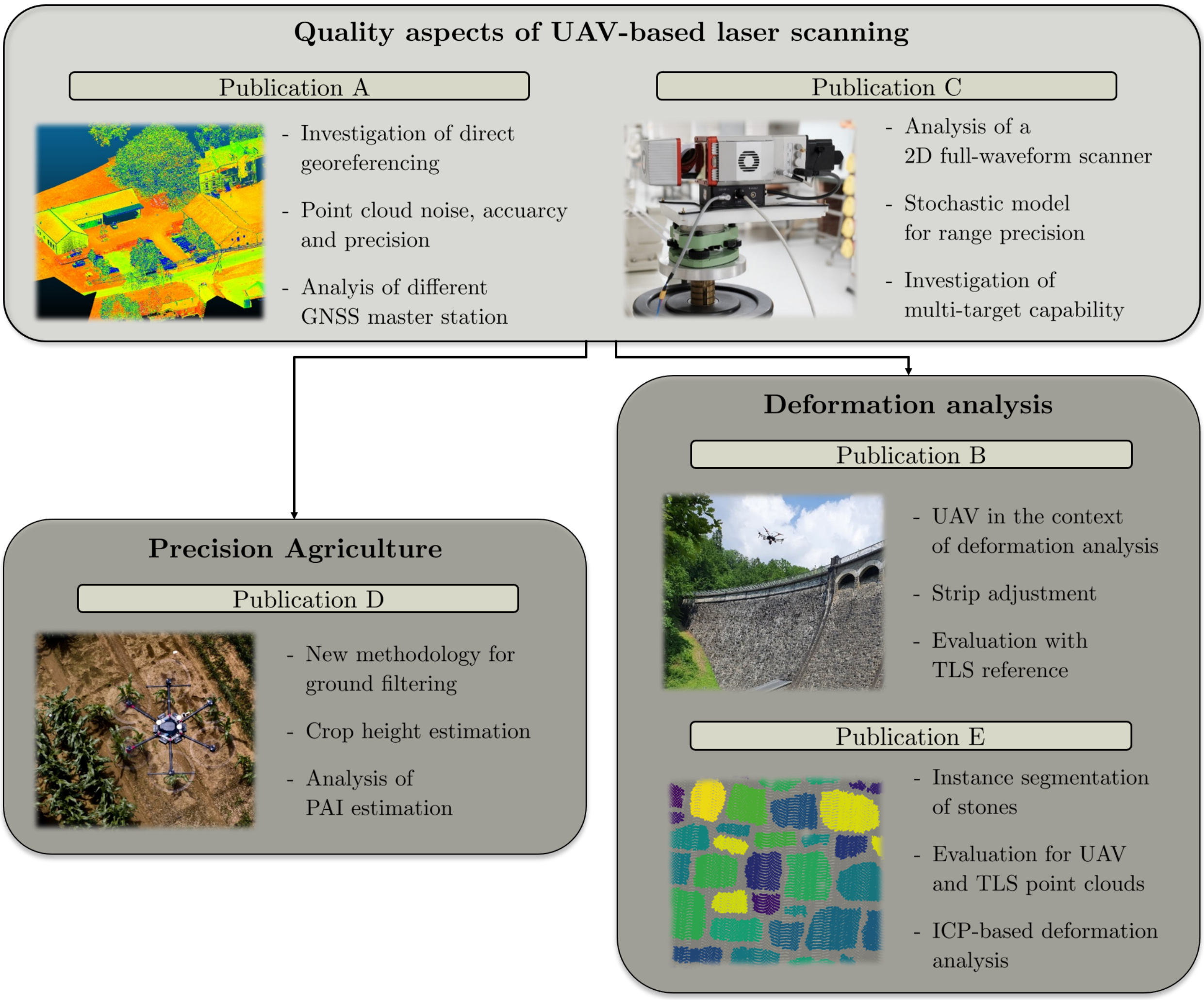

Figure 4.1: Summary of the content of the relevant publications.

of UAV-based laser scanning is done in Publication A, especially considering derived point clouds' precision and accuracy. The separated investigation of the 2D full-waveform laser scanner in Publication C focuses mainly on the range precision and the multi-target capability. Both publications contribute to a better understanding of the multi-sensor system. In Publication D, the UAV-based laser scanning system is used in the context of agriculture to derive the structural wheat traits with crop height and plant area index. In Publication B, the potential of UAV-based laser scanning for deformation analysis of a water dam is evaluated based on a case study and a comparison with a TLS reference point cloud. Furthermore, in Publication E, the captured point clouds of the dam were used for stone instance segmentation that improves the use of ICP matching for deformation analysis. The following sections summarize the content of relevant publications briefly. The main aspects of these publications are addressed in Chapter 5.

Publication A (Peer-reviewed, Journal)

- Dreier, A., Janßen, J., Kuhlmann, H., & Klingbeil, L. (2021a). Quality analysis of direct georeferencing in aspects of absolute accuracy and precision for a UAV-based laser scanning system. *Remote Sensing*, 13(18), 3564

This publication performs the quality analysis of direct georeferencing for a UAV-based laser scanning system using different evaluation strategies. These are separated into four aspects: (1) point cloud noise, (2) accuracy, (3) precision of repeated measurements, and (4) the impact of the GNSS master station used. The results are analyzed using data sets from two different study areas designed for evaluation. The novel aspects compared to existing studies are especially the analysis based on repetitions of the same measurement flight and investigations of results without additional strip adjustment in corridor mapping. Furthermore, the included target-based evaluation strategy enables the evaluation in 3D compared to the typical airborne data assessment based on elevation models.

One advantage of UAV-based laser scanning is the possibility of direct georeferencing, which results in a 3D point cloud in a global reference system. Nevertheless, multiple uncertainty factors influence the quality of direct georeferencing related to trajectory estimation, system calibration, laser scanner, and miscellaneous errors. The quality analysis is based on data sets from two study areas with a corridor mapping without strip adjustment and cross-flight pattern, including additional strip adjustment. The results are related to the multi-sensor system used with a RIEGL miniVUX-SYS, but the evaluation performed is transferable to other sensor systems. Both data sets are evaluated using targets and tables distributed in the study areas. The four aspects (1) - (4) within the paper can be summarized as follows:

(1) The first parameter, which describes the noise and thus a relation with the range precision of the laser scanner, results in $\sigma = 0.4$ cm at an altitude of 10 m for single strip measurements and $\sigma = 0.6$ cm at an altitude of 25 m for the measurement of multiple strips. The methodology uses the residuals of a 3D plane adjustment for noise evaluation. The second data set is also used to assess the performance of the strip adjustment in RIEGL's RiPRECISION software, which correctly aligns multiple strips from the cross-flight pattern.

(2) The accuracy is investigated using the target-based evaluation compared to a TLS reference. For four separate flights, the mean difference was 0.9 cm in the east, 1.9 cm in the north, and 3.4 cm in the height direction for the single strip measurements. The additional focus on the vertical direction using table heights resulted in an almost identical height offset of 3.4 cm with an RMSE of 1.3 cm. The measurement results with multiple strips are consistent with the first data set, with an average difference in the horizontal direction of 1 cm and 4 cm in the vertical direction. An additional parameter-based evaluation was performed based on the tilt of planes, revealing no systematic errors.

(3) The precision of the UAV-based laser scanning system is evaluated based on repetitions of the same flight planning and the following comparison of point clouds. This resulted in a standard deviation of 0.7 cm for the east, 1.1 cm for the north, and 1.2 cm for the height direction using target-based evaluation. The same analysis resulted in a precision of 0.8 cm in the east, 0.5 cm in the north, and 2.1 cm in the height direction for the multiple strip measurements.

(4) The effects of the different GNSS master stations are evaluated by using their own master station, a CORS station, and two different VRS. The target-based evaluation revealed no significant differences between results for the four GNSS data sets. Overall, the VRS and CORS stations showed comparable deviations and are suitable alternatives for processing.

Publication B (Peer-reviewed, Conference)

- Dreier, A., Kuhlmann, H., & Klingbeil, L. (2023a). The potential of UAV-based laser scanning for deformation monitoring - case study on a water dam. *5th Joint International Symposium on Deformation Monitoring (JISDM 2022), Editorial Universitat Politècnica de València*, 2023, 261–269

This publication investigates the potential of UAV-based laser scanning for area-based monitoring of a water dam. The challenges to derive an accurate point cloud in this context are given by trajectory estimation, the suboptimal measurement environment, and flight planning. The main contribution of this work includes the strip adjustment of performed flight patterns and following evaluation based on targets and point clouds using a TLS reference point cloud. The novelty of this study is the use of a UAV-based laser scanning system for the application of water dam monitoring and the discussion of current potential and challenges.

The specialized flight pattern for the coverage of the water dam is based on five parallel flight strips in front of the dam with increasing altitude from 5 - 25 m. The challenging trajectory estimation was evaluated based on satellite geometry and corresponding DOP (Dilution of precision) values as a prior for trajectory quality. It can be assumed that the uncertainty is higher than typical measurement conditions due to the low number of satellites, the very error-prone environment, and the poor satellite geometry. This analysis follows flight strip comparison after direct georeferencing, which shows significant misalignments between consecutive strips. The systematic errors between flight strips are especially present by horizontal shifts in the cm - dm range and slightly lower values in the vertical direction. Furthermore, a systematic tilt due to uncertainties in the orientation is present but not as prominent as the translation. The challenging GNSS conditions explain this. The evaluation of the inner geometry of individual flight strips using target distances showed high consistency.

So far, the analysis was based on results from direct georeferencing without the introduction of ground control points or strip adjustment. Therefore, the strip adjustment minimizing misalignments between flight strips is performed within RIEGL's RiPRECISION software. Next, the registration between TLS reference and UAV was established by estimating the transformation parameters with measured targets. The evaluation between TLS and UAV was based on visual interpretation in the first step, followed by a point cloud comparison using the M3C2 algorithm. The visual inspection provided a good insight if the registration to the same geodetic datum worked correctly due to the structure of joints and stones in the point clouds. The M3C2 provided a quantification of the point cloud quality compared to the TLS with a mean difference of 5 mm and a corresponding standard deviation of 9.2 mm. These results presented the quality in terms of precision for using UAV-based laser scanning but also showed the limiting factors so far if GNSS conditions are challenging.

Publication C (Peer-reviewed, Journal)

- Dreier, A., Jost, B., Kuhlmann, H., & Klingbeil, L. (2024a). Investigations of the scan characteristics with special focus on multi-target capability for the 2D laser scanner RIEGL miniVUX-2UAV. *Journal of Applied Geodesy*, 18(1), 97–113

The error budget in UAV-based laser scanning can be separated into uncertainties related to trajectory estimation, sensor calibration, laser scanner, and miscellaneous errors. This publication analyzes the quality of a 2D laser scanner used in such a multi-sensor system without the sensors for pose estimation. The parameters derived for the 2D laser scanner RIEGL miniVUX-2UAV include the range precision, the rangefinder offset as part of the range accuracy, the resolution capability, and the multi-target capability. The publication focuses on evaluating the multi-target capability, which enables the detection of multiple objects with one laser beam using the full-waveform. The main novelty of this study is the analysis of multi-target capability, in which the relationship between precision and the attribute of pulse deviation is established. In addition, the systematic investigation of the minimum distance between two plane targets is carried out for the first time. In both cases a new measurement setup and methodology is presented.

The range precision of the laser scanner is investigated concerning scan parameters, object materials, distances, and scan geometry with different incidence angles. The range precision is evaluated based on residuals of a line fit and summarized in a stochastic model in relation to the measurement amplitude. Different configurations of scan parameters with changes in scan speed and pulse repetition rate have shown no systematic difference in the resulting range precision. Further investigation resulted in an increasing precision value for larger distances and also larger incidence angles, which is expected based on the LiDAR range equation. Finally, the intensity-based stochastic model is fitted using the entire data set, which fits well with the theoretical model presented by Wujanz et al. [2018].

The second parameter estimated for the laser scanner is the rangefinder offset as part of the range accuracy. This is evaluated with a dedicated measurement setup using a total station as a reference. The offset resulted in values between 8 and 11 mm within the manufacturer's specification. Furthermore, the angular resolution capability describing the ability to distinguish between two specially separated objects is investigated. This is done with a new measurement setup by transferring the existing concept for panorama scanners to the 2D case. The limiting factor is identified with the footprint size. The mean value for the resolution capability in the vertical direction reveals values at about two - three times the footprint size.

The last part of this contribution is the evaluation of the multi-target capability with different research questions. The minimal distance between two objects that can be separated is analyzed empirically with about 1.6 m for the used laser scanner. Furthermore, the dependency on reflection properties for different materials and the corresponding precision of multi-target detection is presented. Increasing separation between two targets leads to higher precision in detecting two echoes. Finally, the systematic relation between precision and the attribute pulse deviation is shown, which creates the possibility of evaluating individual measurements.

Publication D (Peer-reviewed, Journal)

- Dreier, A., Lopez, G., Bajracharya, R., Kuhlmann, H., & Klingbeil, L. (2025a). Structural wheat trait estimation using UAV-based laser scanning data: Analysis of critical aspects and recommendations based on a case study. *Precision Agriculture*, 26(18)

This publication uses a UAV-based laser scanning system to analyze the estimation of structural wheat traits. The parameters under investigation are winter wheat's crop height and plant area index (PAI). The first part presents a novel approach for ground classification using derived point clouds as a pre-processing step for the following parameter estimation. A detailed analysis of plant height and PAI estimation follows in the second part. The entire analysis used a high-temporal data set based on 19 UAV flights. The novelty of this investigation relates to the methodology of ground classification and the analysis of impacting factors for PAI estimation like the ground classification and the extinction coefficient.

The proposed algorithm for ground classification aims to separate two classes with points on the ground and everything else assumed as crops. The approach is based on point cloud features used within a k-means classification. The features are designed using geometric information calculated as a height above the minimum value and the sphericity of the point neighborhood. Furthermore, two radiometric features with the neighborhood's mean pulse deviation and mean intensity are introduced. This pre-classification with k-means was followed by an outlier removal using a polynomial fit in 3D. The evaluation of the approach in comparison to the cloth simulation filter (CSF) has shown better results, especially in the early growing phase, with a specificity of 93.9 % compared to 70.7 % (CSF).

The crop height estimation uses a raster representation to derive the mean plot height compared with manually measured reference heights. Results showed a high correlation between estimated crop heights and reference with a R^2 value of 99.69 %. Nevertheless, a systematic shift with a mean absolute error of 7.4 cm is included. These systematics can be attributed to the interaction between laser pulse and plants, where a resolution of tiny objects is challenging, resulting in measurements within the canopy.

The estimation of PAI is based on the Beer-Lambert law with three different variations. The results generally showed a high correlation with reference values but systematic deviations depending on the used extinction coefficient. The additional introduction of scan angle weighting slightly improved the result. Nevertheless, the best results were achieved in the case where reference values were used for the estimation of the extinction coefficient. In this case, the evaluation resulted in a R^2 value of 97.66 % and a mean absolute error of 0.250. Within the last part, the impact of the gap fraction was evaluated by propagating the uncertainty to the PAI estimate. This evaluation showed the highest impact at the beginning and end of the growing season but a low impact compared to the extinction coefficient.

Publication E (Peer-reviewed, Journal)

- Dreier, A., Tobies, A., Kuhlmann, H., & Klingbeil, L. (2025b). Stone instance segmentation of rubble masonry based on laser scanning point clouds. *Measurement*, 242, 115905

Deformation analysis using laser scanning provides area-based information and enables targeted intervention in case of displacements. The approaches for analysis will be improved if identical areas or objects can be detected in advance. The challenge is to identify the same areas in point clouds from several epochs. If such an identification is successful, this can be used as preliminary information in the deformation analysis. One approach for the estimation of transformation parameters between epochs is the ICP registration based on identical areas. In the application of the water dam, individual stones are analyzed as identical areas which would enable a deformation analysis. This publication presents a new approach for instance segmentation of stones of a water dam built with rubble masonry. The algorithm is evaluated on two data sets with manually labeled reference instances from UAV-based laser scanning and TLS. This also includes an initial deformation analysis using a second epoch with simulated deformations.

The methodology for instance segmentation uses a k-means classification followed by image processing. Within the first step, the measured intensity is used for the first separation between stones and joints. Due to different reflection properties, the intensity values deviate between the different areas. Afterward, the point cloud is projected to an image, and different processing steps are performed, mainly detecting segments with connected component labeling. Based on calculated quality indicators, the segmentation result is evaluated and corrected with the watershed algorithm in cases of wrong segmentation. The instance segmentation of stones was analyzed with reference labels, resulting in 90.82 % correctly identified stones for the UAV data set and 89.29 % for the TLS. Besides the segmentation itself, the individual stone is evaluated by considering its shape and location. The mean area of stones identified by the algorithm compared with the reference is 98.07 % for TLS and 99.87 % for the UAV. Furthermore, the centroids of identified stones are compared with the reference, which showed differences below 3 cm.

The last part of the publication presented the first use of segmented stones for deformation analysis using the ICP algorithm. For this evaluation, a deformation was simulated and estimated afterward using instance segmentation followed by ICP matching. The estimated transformation parameters are close to the simulated deformations, highlighting the potential for introducing segmented objects in other algorithms for deformation analysis.

5. Summary of the most important results

The following sections highlight the most important results of this dissertation that have been included in the presented publications. The results are grouped into four main aspects, taking the objectives from Chapter 1 into account with

- Evaluation of direct georeferencing using UAV-based laser scanning (Section 5.1)
- Investigation of quality aspects of a full-waveform 2D laser scanner (Section 5.2)
- Estimation of structural plant traits based on plant height and PAI (Section 5.3)
- Analysis of UAV-based laser scanning for deformation analysis of a water dam (Section 5.4)

The first two aspects aim to provide a general understanding of quality aspects in UAV-based laser scanning, focusing on direct georeferencing and the laser scanner. The latter two aspects discuss the use in the applications of precision agriculture and deformation monitoring.

5.1 Analysis of direct georeferencing using UAV-based laser scanning

Direct georeferencing provides a 3D point cloud in a global reference frame without the additional use of ground control points. Different uncertainty factors (explained in Section 3) influence the quality of the point cloud. Within Publication A, an evaluation strategy is proposed to investigate the quality of direct georeferencing using point-based and parameter-based evaluation strategies. The analysis is based on two study areas with a typical corridor mapping and additional cross-flight pattern. The novelty of this investigation is the analysis of flight repetitions, different GNSS master stations and the evaluation using targets in the context of UAV-based laser scanning. The results regarding the investigation of precision and accuracy are discussed in Section 5.1.1. Additionally, the impact of the used GNSS master station is analyzed empirically in Section 5.1.2. The investigations in this thesis did not analyze the system calibration in detail since different approaches enable the estimation of calibration parameters in advance or within the strip adjustment process of UAV-based laser scanning.

5.1.1 Investigation of precision and accuracy

The approach for the evaluation of direct georeferencing in terms of precision and accuracy is mainly focused on a point-based evaluation using targets. The accuracy is analyzed in comparison to a reference measurement captured with TLS. Furthermore, precision was investigated using a new strategy to perform the same flight pattern multiple times. Due to the new initialization of the sensor system and a changing satellite geometry, the measurements can be assumed to be independent. The first study area, similar to a corridor mapping, is shown in Figure 5.1 with flight directions and objects divided within the study area. The flight parameters for the corridor mapping are a flight height of 10 m, flight speed of 1 m/s, laser scanner line speed of 55 lps, and four flight repetitions. The average point distance with these parameters is 2.2 cm, resulting

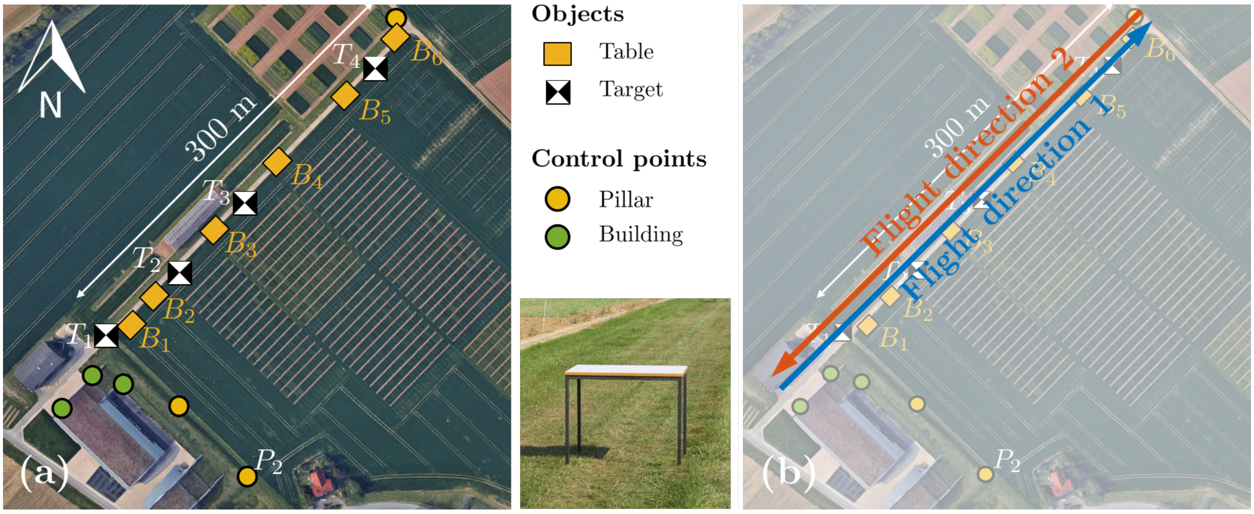

Figure 5.1: Study area for the analysis of single strip measurement with included objects like tables [1.2 m x 0.8 m] and targets [0.3 m x 0.3 m](**a**), and the two flight directions of the individual measurements (**b**), ©`https://www.google.de/maps/`, 14.05.2021

in a point density of 2495 pts/m^2. The TLS scan used for comparison is given with a higher accuracy due to the scan precision, target-based registration and the following georeferencing using control points in the official German coordinate system ETRS89/UTM32. The registration process includes the transformation to geocentric coordinates and therefore the use of ellipsoidal heights for following comparisons. The registration error in relation to the control points was given with a RMSE of 0.5 cm.

The precision analysis used four repetitions of the same flight pattern and four targets distributed within the study area. Each flight included flight direction 1 followed by flight direction 2 in the opposite direction (Figure 5.1). The estimated target centers were used to compute the mean target coordinates $[\mu_x, \mu_y, \mu_z]^T$ with corresponding precision described with standard deviation σ. The target centers are estimated by the algorithm presented in Janßen et al. [2019]. Furthermore, for accuracy evaluation, the differences to the esti-

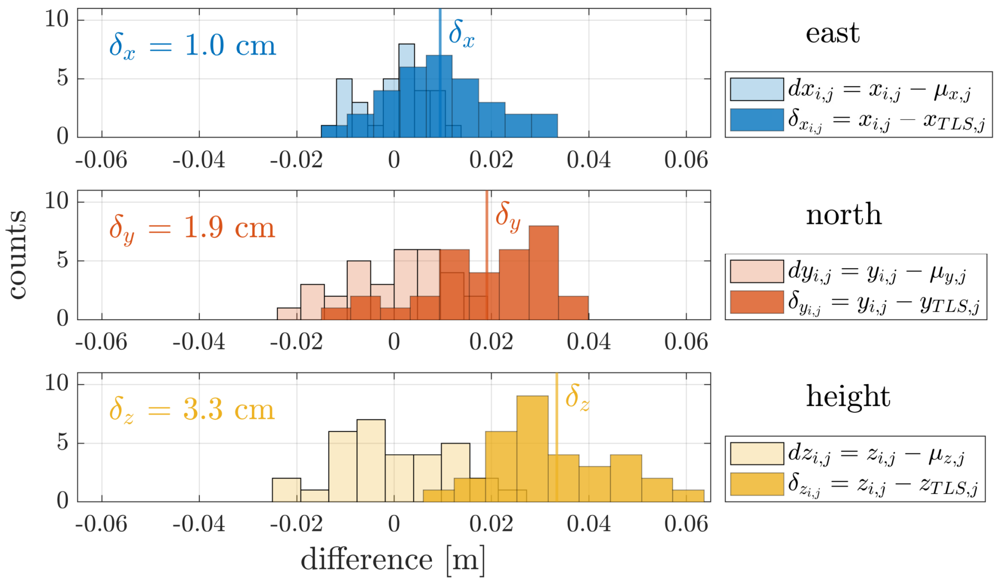

Figure 5.2: Histogram for East, North, and height difference of estimated target coordinates for four flights. Results are separated into estimates for the precision and accuracy compared to the TLS reference.

mated TLS target centers $[x_{TLS}, y_{TLS}, z_{TLS}]^T$ are computed for the four flight repetitions. The histograms in Figure 5.2 provide the summary of the target estimation separated in East, North, and Height directions. The results are shown together for the targets of the four flights with the index i for the corresponding data set and index j for the target number. The accuracy is quantified with the mean absolute difference δ to the TLS reference and corresponding RMSE values. The results for the mean absolute difference in the east direction δ_x is 0.9 cm with an RMSE of 1.1 cm and for the north direction δ_y with 1.2 cm RMSE. The height difference resulted in 3.3 cm for δ_z and an RMSE 1.2 cm, which showed a systematic offset most likely due to uncertainties like system or antenna calibration. Furthermore, the precision quantification based on a standard deviation of target coordinates resulted in values lower than 1.2 cm in all directions. Both results for precision and accuracy confirm the manufacturer's specification for this UAV-based laser scanning system but reveal an offset in height direction.

Due to the systematic offset in the height direction, an additional analysis is presented in Publication A, which uses planar surfaces included in the repetition of the flight pattern. Therefore, a plane fit is used to estimate the height for a given location (east and north direction) of six tables (Figure 5.1). The ellipsoidal heights

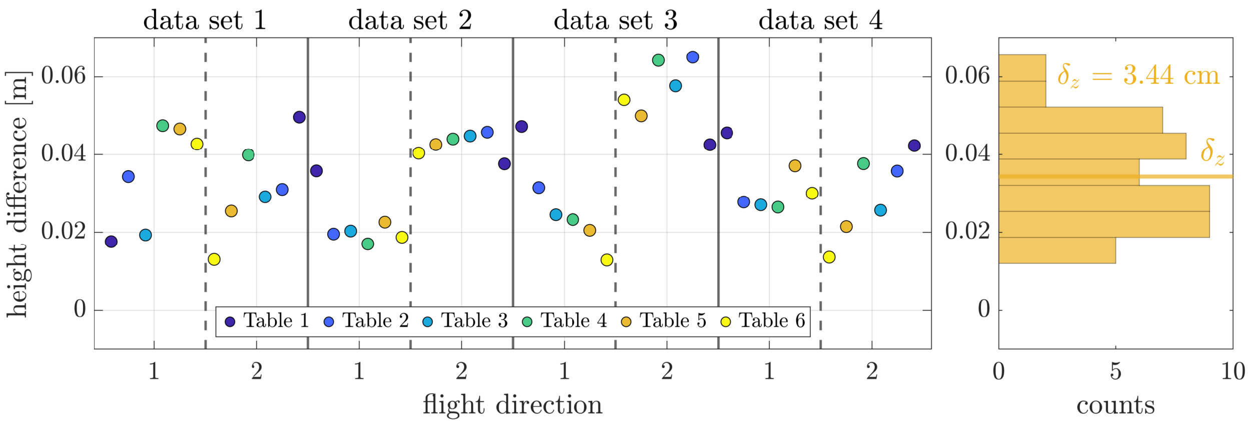

Figure 5.3: Height difference of estimated table heights for four flights.

were compared with the TLS result and plotted for the individual flight in Figure 5.3. Next to the separation in the data sets, the flight direction is also separated as provided in Figure 5.1. The summary of height differences is presented with the histogram on the right, providing a similar systematic offset with 3.4 cm for the four data sets. The corresponding RMSE with 1.3 cm is also similar to the results shown with the target-based investigation. Nevertheless, the analysis here also presents the separation in the flight in both directions and potential changes over the study area. Overall, the values are within the manufacturer's specifications. Moreover, a similar analysis was provided for a second study area with additional strip adjustment for a cross-flight pattern. The analysis regarding precision and accuracy showed a strategy to analyze the direct georeferencing. This flight repetition and analysis approach based on targets and planes can also be used for different sensor systems and study areas.

5.1.2 Empirical analysis of the effects of used GNSS master station

One crucial aspect considering the quality of direct georeferencing is the GNSS baseline processing for trajectory estimation. Since this provides the geodetic datum and the position in the global reference frame, uncertainties propagate systematically in the estimated UAV pose. Within Publication A, the impact of the used GNSS master station is analyzed empirically. The investigation processed the presented data set of Section 5.1.1 with four different GNSS master stations: with their own base station, a CORS station, and two different virtual reference stations (VRS). This comparison provides a new empirical analysis of the

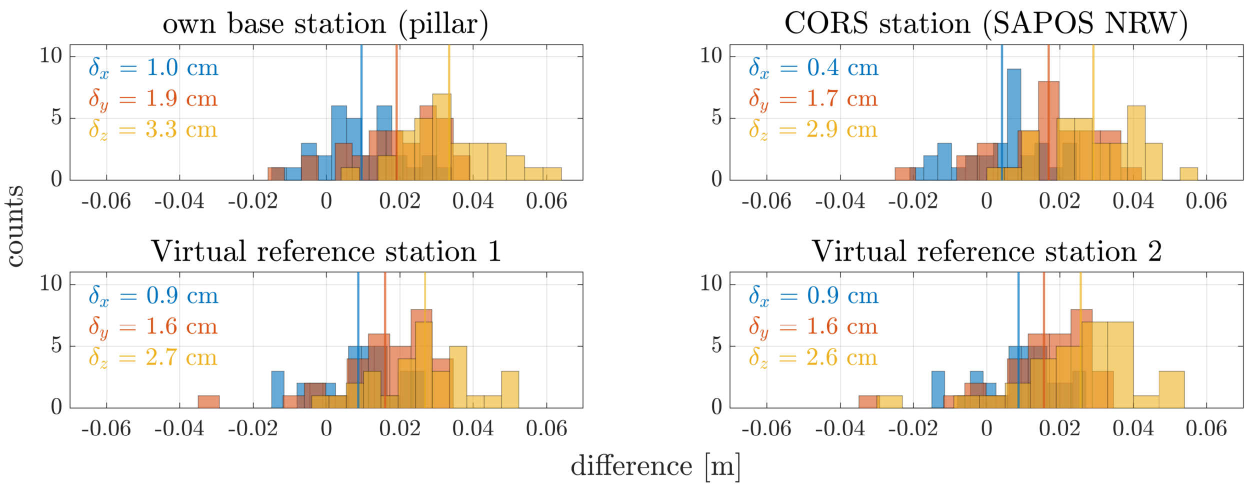

Figure 5.4: Difference of the estimated target coordinates compared to the TLS reference when using different master stations for the trajectory estimation.

impact of the used master station. For each master station, the four flight repetitions were processed, and similar to before, the target centers were used for evaluation in comparison with the TLS. The results are shown in Figure 5.4 with differences for the east, the north, and the height direction and the mean difference. The result of this experiment showed that the differences between the four master stations are very small and do not lead to substantial systematics within the results. The RMSE and the mean absolute difference agreed with differences in the mm level. Overall, the empirically investigated impact of the GNSS master station has shown especially the viable alternative of using a virtual reference station or CORS station with a larger distance compared to the own master station.

5.2 Investigation of quality aspects of a full-waveform 2D laser scanner

While the previous analysis investigated direct georeferencing with all the uncertainties influencing the point cloud, Publication C investigated only the 2D laser scanner RIEGL miniVUX-2UAV. This approach enables a separate analysis of the laser scanner without uncertainty factors such as trajectory estimation or system calibration. The investigation included four aspects: range precision, rangefinder offset as part of range accuracy, angular resolution capability, and multi-target capability. The contributions regarding the range precision are presented in detail in Section 5.2.1 and the analysis of multi-target capability in Section 5.2.2.

5.2.1 Determination and modelling of range precision

The methodology for determination of the range precision has been discussed for 3D and 2D scanners [Heinz et al., 2018; Schmitz et al., 2019; Wujanz et al., 2018; Winiwarter et al., 2020]. In this study, multiple scan lines of a planar surface were captured with the 2D laser scanner and based on the line adjustment, estimated residuals are used for the determination of range precision σ_r. Afterward, an intensity-based stochastic model was estimated using multiple scans with different configurations. This functional model was estimated in dependence on the raw intensity, respectively, of the mean echoes amplitude $\bar{A}$ for each scan. The stochastic model is given by

$$\sigma_r = a \cdot \bar{A}^b + c \tag{5.1}$$

with unknown parameters a,b and c [Wujanz et al., 2018]. Furthermore, the range precision is analyzed with a variation in scan parameters, scan range, incidence angle and material. The first aspect regarding different scan parameters is shown in Figure 5.5 with different settings for PRR and line speed. Both figures are based

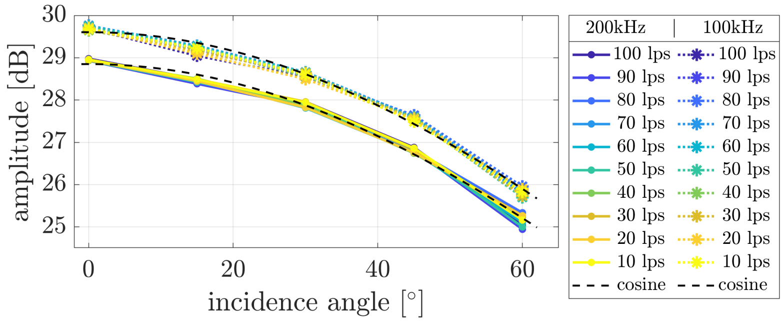

(a) Mean amplitudes for different incidence angles and scan parameters at 22.5 m target distance (wood).

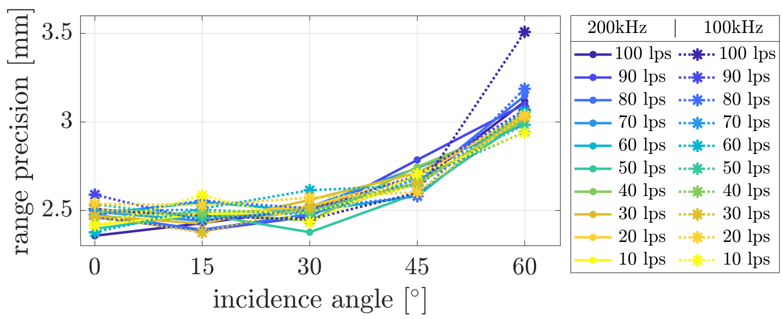

(b) Range precision for different scan parameters at 22.5 m target distance (wood).

Figure 5.5: Impact of different scan parameters on the resulting amplitudes and range precision for different incidence angles.

on the same data set with multiple scans of a wooden target in 22.5 m distance and changing incidence angle. Further, the PRR is set either to 200 kHz or 100 kHz, and the scan speed is varied from 10 - 100 lps with a 10 lps increment. Figure 5.5a presents the dependency of scan setup and resulting amplitudes with a systematic offset of about 1 dB between the different PRR configurations but independent of the incidence angle. This result showed that the lower repetition rate can be measured with a higher amplitude and signal intensity. Figure 5.5b provides the corresponding precision σ_r with values between 2 mm - 3.5 mm and larger values for increasing incidence angles. The previously visible difference between PRR's regarding the amplitude resulted in similar values for the range precision. This result was positive for this scanner, as the hypothesis of the dependency between the scan parameters and the resulting distance precision was disproved [Heinz et al., 2018].

Additional investigations were performed to derive an intensity-based stochastic range precision model, which was evaluated using different materials, scan range, and incidence angle. The results are summarized in Figure 5.6 with an additional plot of the fitted model given with Equation 5.1. The stochastic model showed a good agreement with the data from the different investigations regarding scan geometry, materials, scan parameters, and different scan ranges.

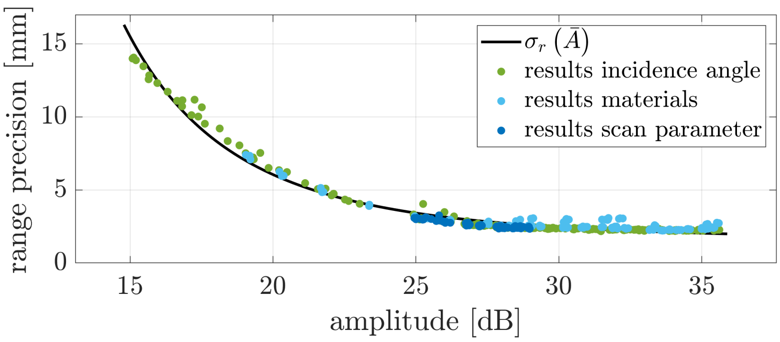

Figure 5.6: Stochastic model for range precision based on raw amplitudes for the RIEGL miniVUX-2UAV.

5.2.2 Analysis of multi-target capability

Publication C investigated a new approach for the empirical analysis of the multi-target capability. Next to the design of a dedicated measurement setup, different research questions were discussed for the detection of two targets. The aspects are separated into the detection of multiple echoes regarding the minimal distance between targets, the precision of detected echoes, and the relation to scanner attributes like amplitude or pulse shape deviation. Furthermore, the study included two different measurement setups with one at a

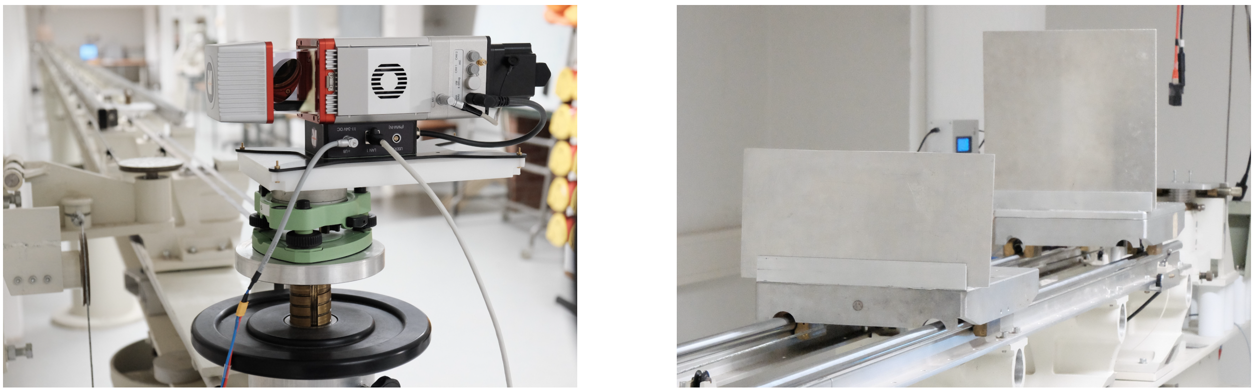

(a) Mounting of the 2D laser scanner RIEGL miniVUX-2UAV for measurements.

(b) Two aluminium targets used within the multi-target investigation.

Figure 5.7: Measurement setup for multi-target capability investigation on the comparator track.

comparator track (as shown in Figure 5.7) and afterward transferred to larger scan ranges outdoors. For the first aspect of the minimal distance between two targets, the separation between the two planar targets (Figure 5.7) is changed between measurements. Therefore, a systematic investigation was possible with a fixed second target at 22.5 m and a change in separation between targets by moving the first target. The first detections of multiple echoes were recorded with a separation of about 1.6 m, which was higher than the theoretical minimum of 90 cm derived from the laser pulse length. Next to this, a systematic increase in the number of detected multiple echoes was visible with increasing separation between the planar targets. This relation was also to be expected since, with increasing separation, the reflection from both targets can be better separated within the full-waveform recording.

The second aspect analyzed the precision of the multiple echoes since the first aspect only considered the overall detection without the quality of the detected pulses. To investigate this, the echoes are assigned either to the first or the second target in the first step and evaluated regarding the reference distance. By using an additional threshold of $3\sigma_R$ based on the manufacturer specification ($\sigma_R = 10mm$), the echoes are assigned as inlier or outlier. One example of the evaluation is shown in Figure 5.8 with absolute residuals of multiple

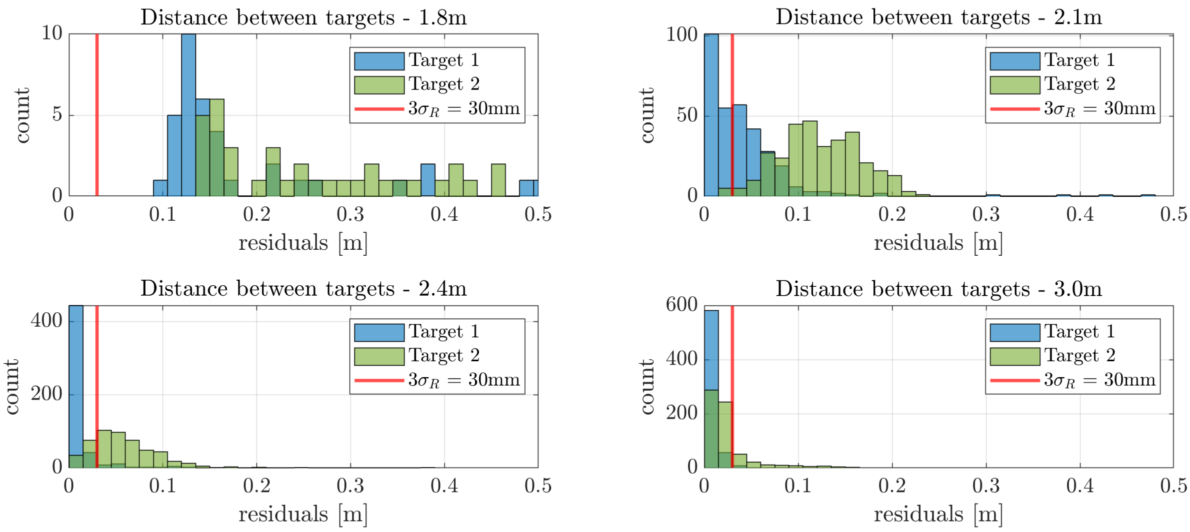

Figure 5.8: Residuals of multiple echoes for the first target (blue) and the second target (green). The second target is always in a distance of 22.5 m, whereas the first target is changed, resulting in a distance between targets between 1.8 m - 3 m.

echoes regarding the reference distance. For the four different plots, the second target is always placed at a distance of 22.5 m while the first target location is varied to achieve a separation between targets of 1.8 m, 2.1 m, 2.4 m, and 3.0 m. These results showed two main aspects. First, the residuals to the reference targets are getting smaller with increasing separation between targets. Secondly, the echoes on the first target are always more precise than the second one. The shown evaluation from the comparator track was transferred to an outdoor experiment with larger distances up to 100 m and a similar measurement setup, which is summarized in Figure 5.9. In this case, only the percentage of inliers is plotted with the separation between

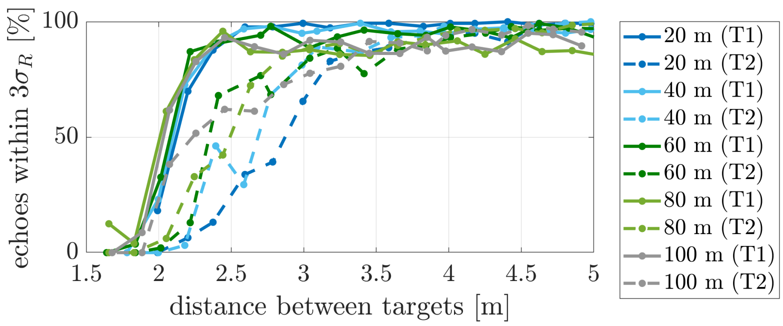

Figure 5.9: Percentage of multiple echoes evaluated as inlier based on $3\sigma_R$ filtering.

both targets. This result again showed the higher precision of echoes on the first target compared to the second target, and with increasing separation between targets, multi-target detection improved. Within the last aspect, the investigations were analyzed regarding the amplitude and pulse shape deviation scan attributes to derive a relation between multiple echoes and each measurement. Regarding the signal amplitude, the investigation showed a better separability of two echoes in cases where the amplitude is similar, especially when the separation between targets increased. The pulse shape deviation has shown an even more systematic relation as shown in Figure 5.10 with mean pulse shape deviation in relation to the distance between two targets. As discussed, the increasing separation between targets led to a higher percentage of inliers. The pulse shape deviation, as a measure of the quality of the reflected signal, showed smaller values with increasing separation between targets. Therefore, the deviation attribute can be used as a quality indicator even for multiple echoes in practice.

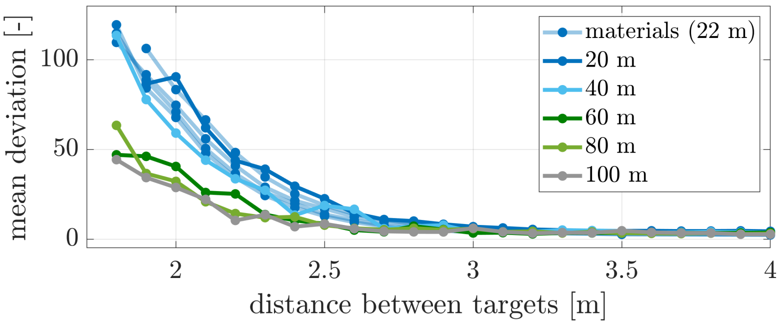

Figure 5.10: Mean pulse shape deviation attribute in dependency to the separation between targets.

The most important innovation of this study is the analysis of multi-target capability, where the relationship between precision and the attribute of pulse shape deviation is established. Furthermore, a systematic investigation of the minimum distance between two plane targets is carried out for the first time. In both cases, a new measurement setup and a new methodology are presented.

5.3 Estimation and analysis of structural plant traits

One potential application of UAV-based laser scanning is precision agriculture, which can be used to derive various plant traits. Within Publication D, the derivation of structural wheat traits is analyzed, focusing on the crop height and plant area index derivation. The experiment used for the evaluation is the PhenoRob field in 2021, as shown with a small section in Figure 5.11. The following evaluation of the crop height in

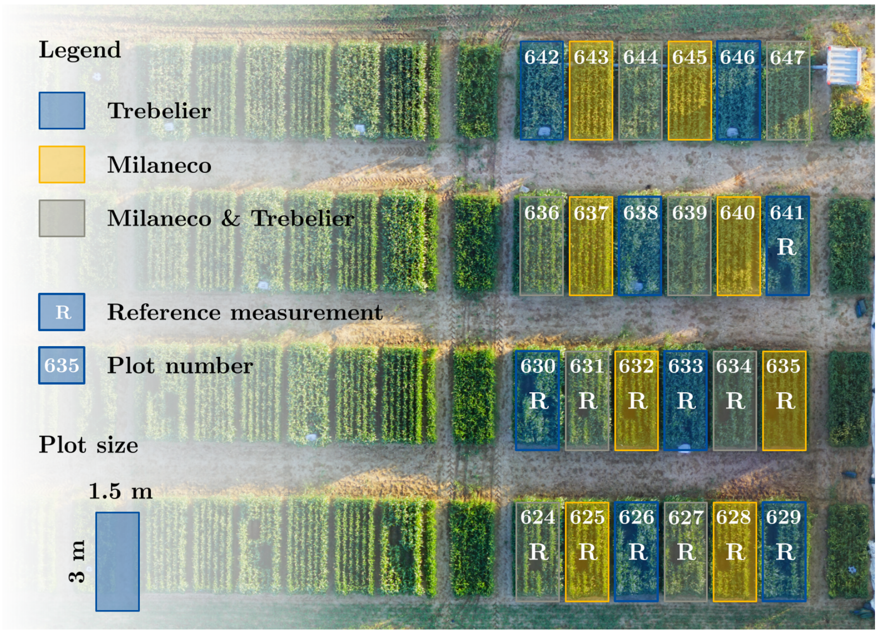

Figure 5.11: Section of the PhenoRob field experiment 2021 at the Campus Klein-Altendorf.

Section 5.3.1 and plant area index in Section 5.3.2 used 19 UAV flights, mainly covering the field's winter wheat part. Reference data measured in the field is available to evaluate the derived crop traits. One crucial aspect of evaluating the point cloud and following the estimation of the parameters is the interaction between the laser pulse and the objects. Therefore, this publication discusses the results of the resolution capability from the detailed investigation of the 2D laser scanner in Publication C with the ability to detect small plant structures in the early growth phase.

5.3.1 Crop height

The crop height is one of the parameters for monitoring the crop status and health for farmers or within breeding experiments. The used approach for crop height estimation is provided within Figure 5.12. Within

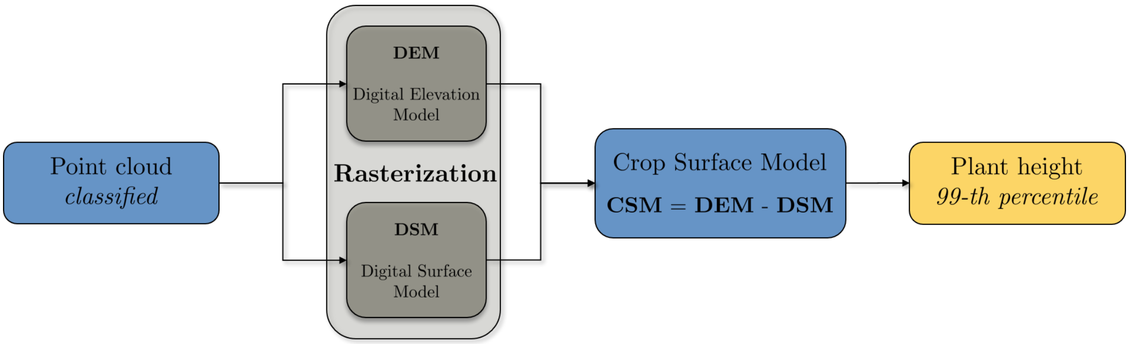

Figure 5.12: Approach for crop height estimation based on the 99th percentile of the crop surface model.

the first step, the point cloud is classified into points on the ground and the crop, which is done in a pre-processing step. In Publication D a novel approach based on k-means classification using geometrical and radiometrical features is presented for this task. This ground filtering starts with the calculation of the features for each point using a defined local neighborhood. The applied k-means classification is followed by geometric filtering to filter outliers. For geometric filtering, an approximated surface parameterized using polynomials followed by a residual-based outlier filtering is applied. With this step, the classification of the point cloud in soil and crop is finished. Based on the following rasterization, the Crop Surface Model (CSM) is derived by describing the relative height referenced to the elevation model. This result can already be used for area-based analysis of the estimated crop height. In this context, one highlighted advantage of UAV-based laser scanning is the derivation based on a single measurement flight, as shown in this study's results. Since the laser can penetrate the crop canopy, it is possible to capture the soil even in later growing stages, which is typically not true for photogrammetry.

The results for crop height estimation for different varieties are presented in Figure 5.13 with R^2 plot showing the comparison with four reference measurements. Furthermore, Figure 5.14 presents the time series of crop

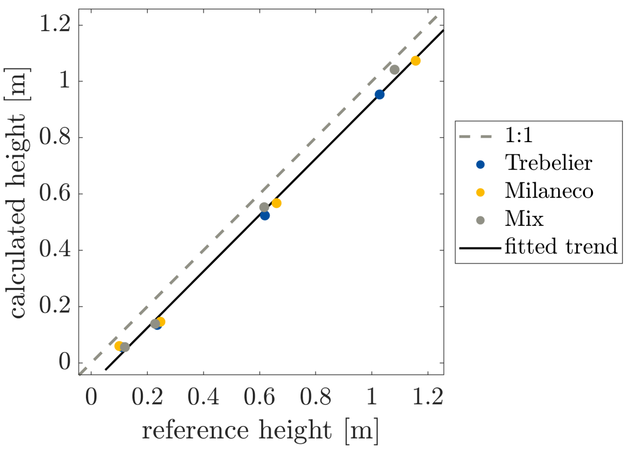

Figure 5.13: Reference against calculated crop heights.

heights for the Trebelier variety and the additional fit of a logistic function as a representation of the plant growing. The results are computed for individual plots (single plot) on the field based on the 99-th percentile of heights. For comparison with the reference measurements, the mean value of multiple heights is used.

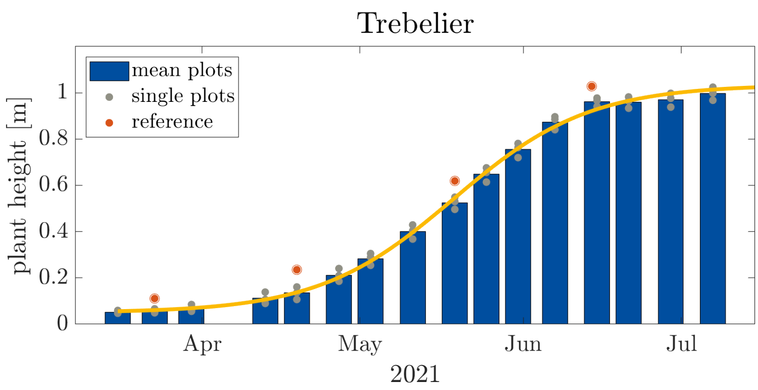

Figure 5.14: Crop height time series of variety Trebelier.

Based on the R^2 value of 99.69 % the precision of estimated crop heights in comparison with the reference is highlighted. Nevertheless, the mean absolute error of 7.4 cm for the entire data set indicates an offset between both with lower heights derived with UAV-based laser scanning (Figure 5.13). The reason for this offset can be related to the laser scanner and the resolution capability as a limitation of object size, which can be resolved. Since most parts of the crops are smaller than the footprint of the laser pulse, the reflected signal is likely a mixture of different reflections, resulting in systematically longer range measurement. Overall, the investigations showed the potential for using UAV-based laser scanning for crop height monitoring providing the entire processing and evaluation based on reference data.

5.3.2 Plant area index (PAI)

The Leaf Area Index (LAI) is defined as the leaf area per ground area and is a typical quantification of the development state of crops. In the context of UAV-based laser scanning, it is typically approximated with the Plant Area Index (PAI) since there is no distinguishing between leaves and stems [Bates et al., 2021]. The approach for PAI estimation based on the Beer-Lambert law was investigated in detail in Publication D. The basic idea is the comparison of measured points on the crop with points on the ground. If a higher number of laser pulses propagate through the crop canopy to the surface, there will most likely be a lower value for the plant area. The final estimate developed from the point cloud is calculated using

$$PAI \approx \frac{1}{N} \sum_{i=1}^{N} -\frac{\cos(|\bar{\theta}_i|)}{0.5} \ln\left(\frac{n_{b_i}}{n_i}\right) \tag{5.2}$$

with additional weighting of scan angle θ_i in N classes [Dreier et al., 2025a]. Further, the calculation needs a classification of the point cloud in points n_b related to the ground and the total number of points n. The pre-processing step is done using the same approach mentioned for the crop height.

The novel analysis within Publication D presented new insights and detailed discussions about different estimation approaches for PAI, the extinction coefficient, and the impact of classification results. This section presents only the results for the final estimation approach and a comparison with reference data. Based on Equation 5.2, the PAI was estimated for the same set of varieties as for plant heights. With the variation of extinction coefficient k (given with 0.5 in Equation 5.2), the RMSE values of estimated PAI compared to reference LAI is shown in Figure 5.15b and the corresponding R^2 plot in Figure 5.15c. The use of $k = 0.5$ is prior value coming from literature but is typically not accurate for different crops and measurement conditions [Bates et al., 2021]. It has been shown that the additional adaptation of the extinction coefficient deviating from the default value of 0.5 corrects systematic errors. The minimum RMSE, therefore, provided the best k value for the used data set, with a minimum of 0.905 for Trebelier and Milaneco and 1.07 for Mix plots. Using the corrected extinction coefficient, the comparison of the results in Figure 5.15c showed an R^2 value of 97.66 % and a mean absolute error of 0.25. The presented correction of the extinction coefficient has shown consistent results with high precision. Nevertheless, the coefficient is assumed to be constant so far, which may not be correct as parameters like leaf angle distribution are most likely changing during the growing season.

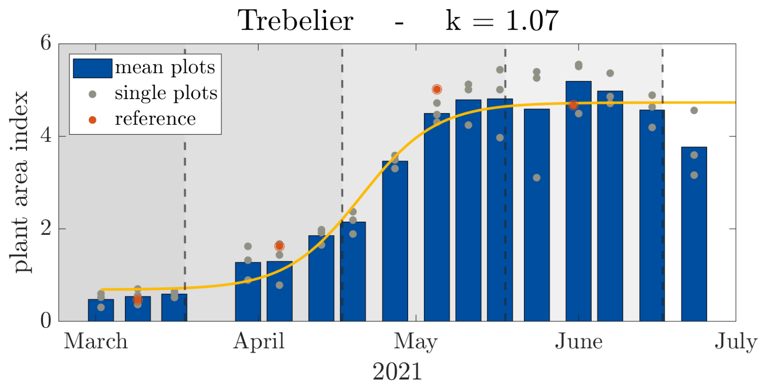

(a) PAI time series for variety Trebelier using $k = 1.07$.

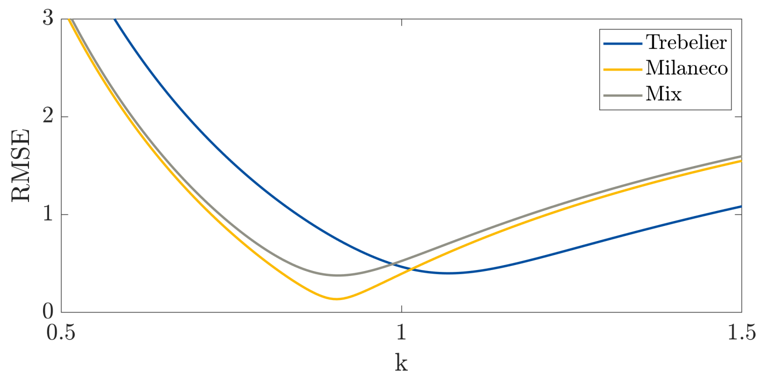

(b) RMSE for PAI depending on the extinction coefficient k.

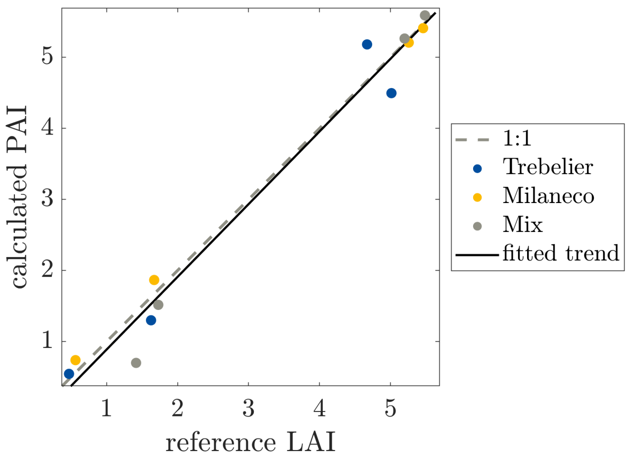

(c) Reference against calculated PAI.

Figure 5.15: PAI results with estimated extinction coefficient k.

Finally, the time series of PAI estimates is shown in Figure 5.15a exemplarily for the entire data set, including multiple plots and reference data. This includes the fit of a logistical function representing the growing stages of the crops. The scattering due to included uncertainties can be seen with the additional plot of the results for single plots. Next to choice of the extinction coefficient k, the uncertainty due to the measurement process and the soil classification are included. Nevertheless, the estimated PAI fit well with the reference data. One aspect analyzed within Publication D is the impact due to the classification step, referred to as the gap fraction in Equation 5.2. This impact is the highest in the early and latest growing stages due to the challenges in classification. Overall, the uncertainty due to the classification is much lower than the errors coming from the choice of the extinction coefficient. This investigation overall shows a new detailed investigation of impact factors for PAI estimation from point clouds with a focus on extinction coefficient and ground filtering impact.

5.4 UAV-based laser scanning for deformation analysis of a water dam

The use of UAV-based laser scanning in the context of deformation analysis can have high demands considering the quality of the point cloud, e.g., in terms of accuracy. Within Publication B, the application of UAV-based laser scanning in deformation monitoring at a water dam is investigated. In addition to a new flight pattern for capturing the water dam, the point clouds are compared to a TLS reference, which is presented in Section 5.4.1. In deformation analysis with point clouds, multiple scan epochs from the same object are captured. Different approaches like the M3C2 algorithm [Lague et al., 2013] are available for comparison. In cases where identical corresponding regions of the point clouds are detected in advance, the deformation analysis could be even further advanced. For this purpose, the result of the instance segmentation of rubble masonry stones developed in Publication E is presented in Section 5.4.2.

5.4.1 Quality analysis of UAV-based laser scanning for deformation analysis

Compared to other areas of application, the measurement environment at a water dam can be more challenging. The additional aspects that have to be considered are specialized flight planning and relatively unfavorable GNSS conditions. Both aspects can lead to larger uncertainties within the trajectory estimation, which can decrease the point cloud's quality. The point cloud is compared to a TLS reference in Publication B with different research questions to evaluate the potential of using UAV-based laser scanning in water dam monitoring. The first new aspect was the specifically designed flight pattern to capture the water dam with high spatial resolution. The used flight pattern is shown in Figure 5.16 with multiple flight strips, including a changing flight height. Further questions answered in Publication B are the analysis of direct georeferencing quality, the registration between TLS and UAV for evaluation, and the quantification of differences. The main challenge was identified with the trajectory estimation. As the first indication for the quality of trajectory estimation, the satellite numbers and corresponding PDOP values were analyzed with high values for the beginning of the trajectory (PDOP > 2) but improved with increasing flight height. Afterward, the direct georeferencing of scans was used to show the precision between flight strips, resulting in systematic offsets in cm - dm magnitude. Nevertheless, the inner geometry is evaluated additionally based on inter-target distances, providing substantially better results.

Additional strip adjustment was performed in RIEGL's RiPRECISION to improve the point cloud, especially the consistency between flight strips. The evaluation of the strip adjustment has shown that besides the higher uncertainties of the estimated trajectory, the very similar scan geometry and structure of the object are not ideal for the strip adjustment. Therefore, processing one consistent point cloud for the entire data set was not possible. For this, the initial trajectory would need to be better, which might be possible by introducing additional sensors or information into the processing. The evaluation of the UAV point cloud was based on the comparison with a TLS reference point cloud. Therefore, the target-based registration to the same

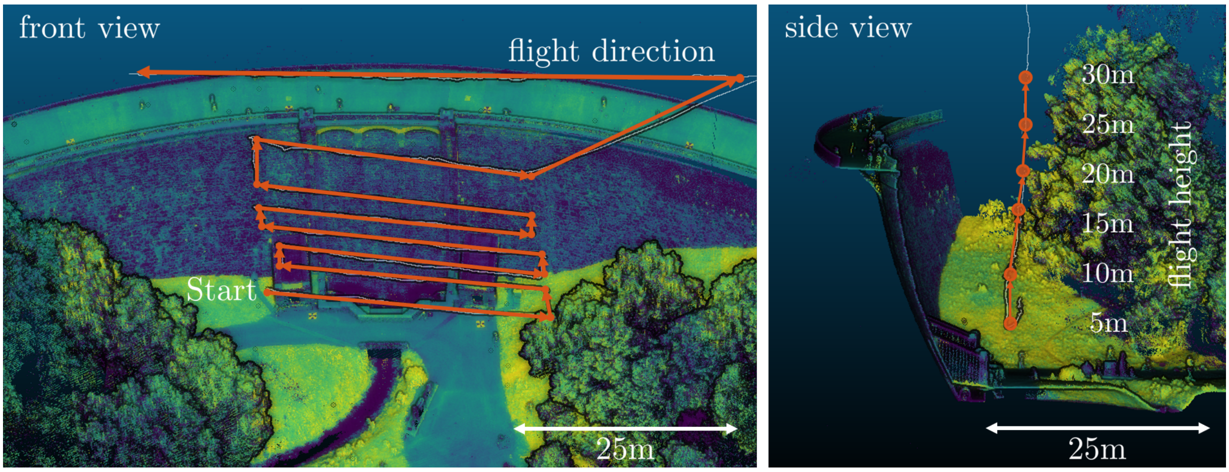

Figure 5.16: Flight pattern performed with the UAV-based laser scanning system in front view (left) and side view (right).

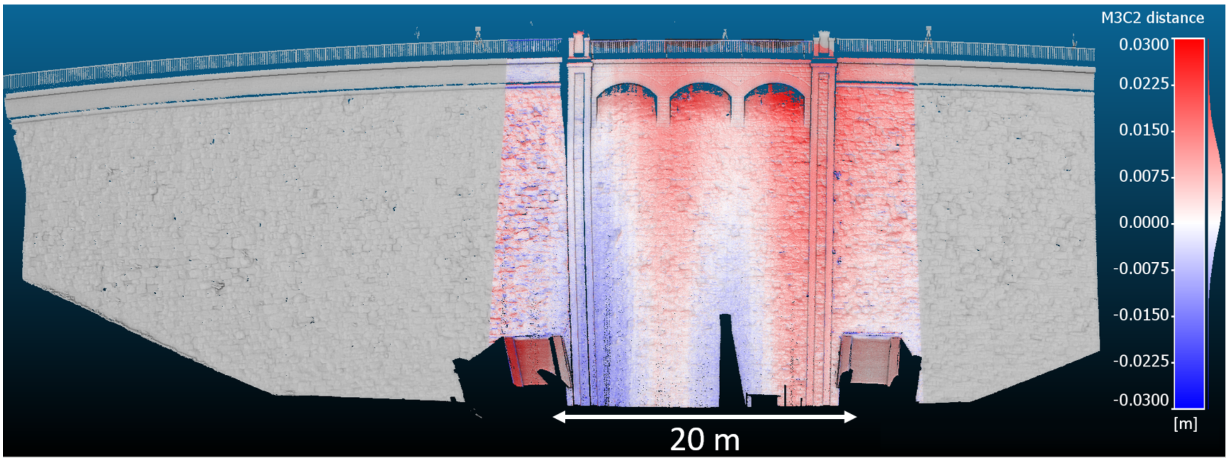

Figure 5.17: M3C2 distances between UAV point cloud from 20 m flight strip and TLS.

geodetic datum was done in the first step. Afterward, one of the flight strips was compared with the TLS point cloud using the M3C2 algorithm. The result is shown in Figure 5.17, where only the colorized areas were captured with both sensors. The mean difference between both point clouds is 5 mm with a standard deviation of 9.2 mm. The comparison still showed systematic effects in different areas of the dam that can be attributed to remaining errors in the trajectory. Nevertheless, the analysis within this publication has shown a new flight planning and processing at a water dam highlighting the different challenges in this application.

5.4.2 Stone instance segmentation in laser scanning point clouds

The previously shown point clouds of a water dam structure can be used for deformation analysis if multiple epochs are available. For this purpose, different methodologies were developed (e.g., M3C2), which can be further improved if identical regions of the water dam were detected in advance. The developed algorithm in Publication E is a stone instance segmentation evaluated with point clouds from TLS and UAV-based laser scanning. The potential use in deformation analysis is presented by the detection of simulated deformation using instance segmentation and ICP matching. The processing steps are shown in Figure 5.18 with examples of intermediate steps based on a 5x5 m point cloud patch. Since the main contribution of Publication E is the development of the segmentation algorithm, it is explained shortly with the individual steps (1) - (6).

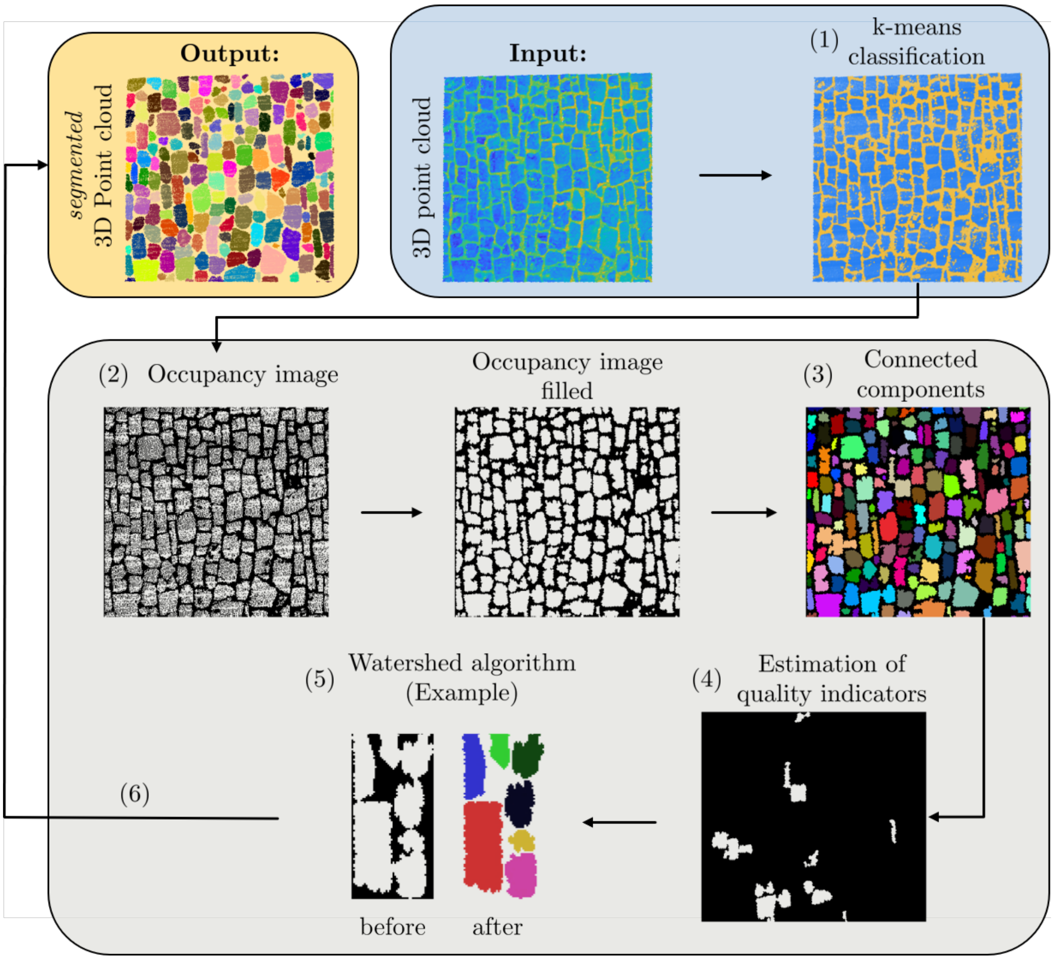

Figure 5.18: Steps of instance segmentation with a 5x5 m patch example.

Step (1) is the use of the k-means classification using the intensity of each point within the region of interest. The classification separates stones and joints, which enables an initial classification since the reflection properties deviate between both. Afterward, step (2) projects the 3D point cloud into a binary image representation with a value of one for the stone pixel while everything else is zero. The following steps are image-based processing algorithms, starting with the connected component algorithm in step (3). With this approach, the first instance segmentation is performed. Since there might be not correctly segmented steps, two quality indicators were designed to identify the problematic stones in step (4). Most of the stones that are not correctly segmented are a group of multiple stones segmented as one instance. Therefore, step (5) performs the watershed algorithm for the separation of multiple stones with small connections. Within the last step (6), the segmentation result is matched back from the image to the 3D point cloud.

For evaluation of the approach for instance segmentation, two point clouds are used that were captured with UAV-based laser scanning and TLS, which are labeled manually to evaluate the algorithm. The reason for both sensors was the assessment of whether the approach could handle different point cloud properties, e.g., regarding spatial resolution. For evaluation of segmentation results, different cases of segmentation shown in Figure 5.19a were covered and presented in Table 5.19b. The most important case is the (a) one-to-one match between the algorithm and the reference, where the segmentation is correct. Every other case of (b) - (e) is wrongly segmented. Next to the presented statistics, the segmentation based on the one-to-one evaluation is shown in Figure 5.20 with additional RGB image for the TLS and the UAV data set. The correctly segmented stones for the TLS data set were 1092 stones (89.29 %), and for the UAV data set, 1128 (90.82 %). The limitation of the segmentation approach so far is given due to the high dependency on

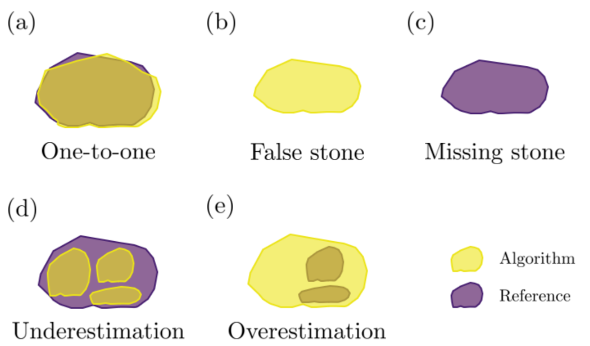

(a) Possible segmentation results of stones.

	TLS	UAV
reference	1223	1242
algorithm	1164	1161
(a) one-to-one	**1092**/1164 (93.81%)	**1128**/1161 (97.16%)
(b) false stone	**10**/1164 (0.86%)	**4**/1161 (0.34%)
(c) missing stone	**12**	**61**
(d) underestimation	**11**/1164 (0.94%)	**3**/1161 (0.26%)
(e) overestimation	**51**/1164 (4.38%)	**26**/1161 (2.24%)

(b) Statistics of instance segmentation.

Figure 5.19: Evaluation of instance segmentation in comparison between reference and algorithm.

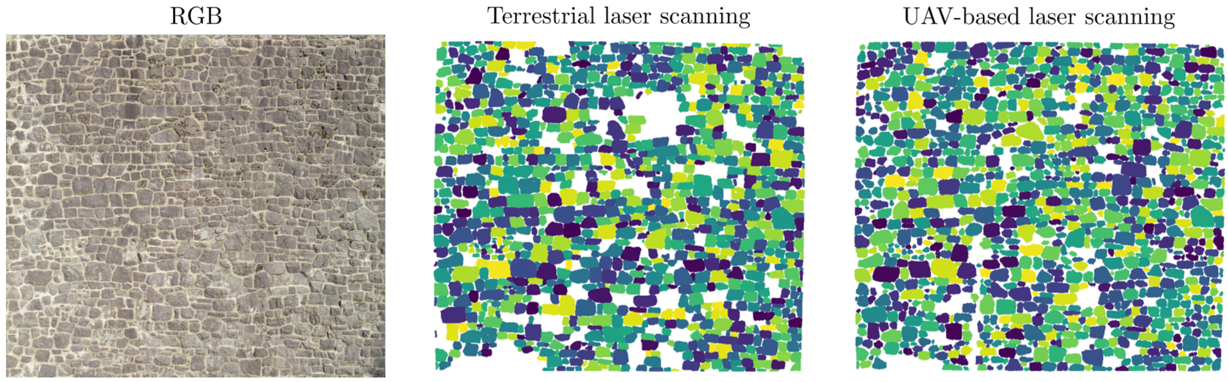

Figure 5.20: Results of instance segmentation for the one-to-one correspondences after evaluation (TLS - 89.29 % and UAV - 90.82 %).

intensity values, which can be used to provide a good initial classification between stones and joints. This is, for example, not the case if areas are wet or overgrown, leading to similar intensities that cannot be used for the separation. Nevertheless, the segmentation result of about 90 % for both data sets is already promising.

Next to the general evaluation of segmentation, the geometry of each stone was evaluated based on the detected point number, the area of the stone, and the 3D position of the centroid in comparison to the reference. The result of centroid evaluation for the UAV data set is shown in Figure 5.21 with the differences between centroids. In this case, the xy-coordinates are the directions in the plane and the z-coordinate is

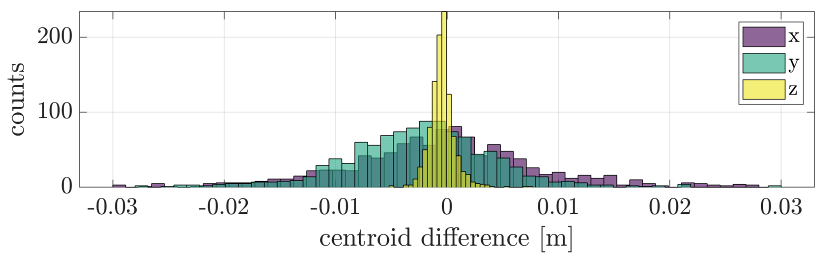

Figure 5.21: Histogram of centroid differences for UAV data set between reference and instance segmentation.

the depth direction. The differences do not show systematic and mean values are next to zero for the UAV data set (0.05 cm, -0.24 cm, -0.04 cm) but also the TLS data set (-0.11 cm, -0.09 cm, -0.01 cm).

Next to the more detailed evaluation, Publication E presented a first deformation analysis based on the instance segmentation. The UAV point cloud was used to simulate a rigid deformation of a few cm. Afterward, the instance segmentation was applied to the initial point cloud and the deformed epoch. With segmented and matched stones from two epochs, an ICP matching for each pair of stones was performed and evaluated with the simulated deformation. It showed that the estimation of the deformation vectors with the ICP was already in the magnitude of millimeters compared to the reference values. This part is also mentioned in the next Chapter about potential future work. Nevertheless, this approach is sensitive if the stone size is very small or the segmentation is incorrect from different epochs. In such a case, using multiple stones for the matching might lead to better results.

6. Further considerations

This thesis deals with the analysis of quality aspects of UAV-based laser scanning with applications in deformation monitoring and agriculture. However, some aspects of the analysis provide the potential for improvement and further research questions. Two potential aspects are discussed: (1) the improvement of trajectory estimation and evaluation and (2) the use of stone segmentation in the context of deformation analysis.

The analysis of quality aspects of UAV-based laser scanning in Section 5.1 and 5.4.1 has shown the potential based on the evaluation of derived point clouds. Nevertheless, the uncertainty of the trajectory estimation within the error budget has been shown as the limiting factor, especially in measurement environments with bad GNSS conditions like the water dam example. There are already different approaches to improve the result using strip adjustment or ground control points [Glira, 2018], but there is still potential for improvement. The quality in terms of accuracy will be improved if the initial trajectory estimation is enhanced. One possibility has been shown by Pöppl et al. [2024] with a comprehensive approach for estimating the trajectory using IMU, GNSS, and laser scanning measurements at the same time. Another approach is the additional use of total station tracking, which provides higher accuracy, especially in a GNSS-denied environment. The first test was already performed with the setup shown in Figure 6.1 with a 360° prism adapted to the UAV-based laser scanning system and the total station. Additional challenges that have to be handled by the use of a total station are time synchronization and the lever arm between the prism and IMU. If this is considered properly, a comparison with the trajectory can be performed as shown with the difference

Figure 6.1: Scanning of a water dam with UAV-based laser scanning including the prism tracking with a total station.

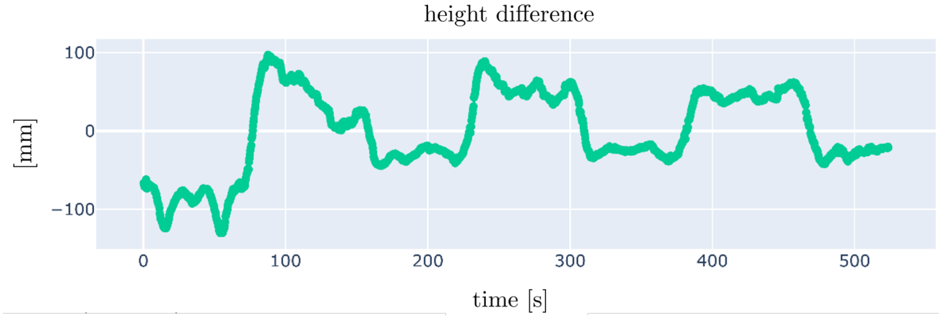

Figure 6.2: Comparison of estimated trajectory with the prism tracked by the total station as the difference in the height direction.

of the height direction for a flight at the water dam in Figure 6.2. This first result is calculated using the methodology described in Tombrink et al. [2024] and shows the errors in the height position with several cm of the trajectory without the use of strip adjustment (as used in Section 5.4.1) . This shows especially the challenge of direct georeferencing in environments with bad GNSS conditions and possible errors resulting in the pose estimation. Tracking the prism enables the trajectory evaluation, which can be used to assess the point cloud's quality. Besides the potential of evaluation, the tracked prism could also be used in the trajectory estimation (e.g., Kalman filter) as additional observation.

The algorithm for stone instance segmentation in Section 5.4.2 provides the possibility to detect identical objects within multiple epochs. The potential of deformation analysis was shown in Publication E with a simulated deformation using the ICP algorithm. The simulated displacement of the entire point cloud with 5 cm, 3 cm, and 1 cm in x-, y- and z-direction was estimated by ICP matching of single stone instances of two epochs. The result is shown in Figure 6.3 with a visual representation of estimated transformation vectors and the corresponding histogram. This result already indicates the potential with mean transformation

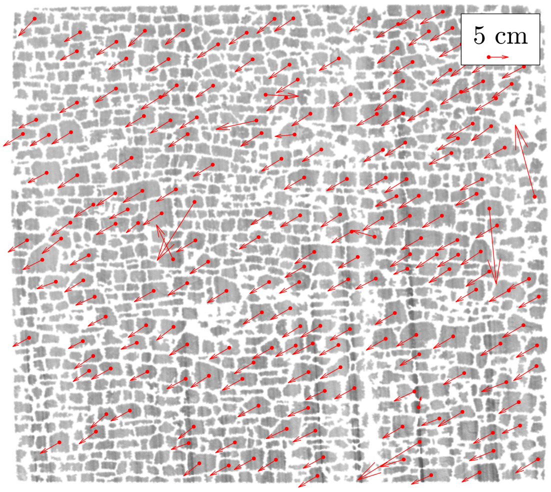

(a) Transformation vectors based on ICP matching.

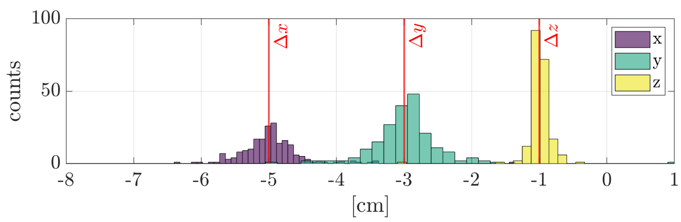

(b) Histogram of estimated ICP transformation parameters.

Figure 6.3: ICP-based deformation analysis using stone instance segmentation. The second epoch is simulated with a deformation of [5,3,1] cm for a point cloud captured with UAV-based laser scanning.

parameters for 200 stones of (-4.89 cm, -2.86 cm, -0.97 cm) close to the simulated deformation. Nevertheless, this provides further potential for future research. First of all, the approach could be transferred to a real measurement of two epochs. Furthermore, the uncertainty of the individual epoch could be taken into account for algorithms in deformation analysis to provide a statistical test of the difference between epochs. Besides its use in the context of deformation analysis, stone instance segmentation could also be used for tasks like registration or calibration of sensors since the same object can be detected in multiple measurements.

7. Conclusions

The processing of UAV-based laser scanning combines various uncertainties propagating to the 3D point cloud using direct georeferencing. If the point cloud is used for the derivation of models or parameters, profound knowledge about the error budget is necessary to assess the results correctly. The main parts within the error budget are typically grouped into the errors in trajectory estimation, system calibration, and the laser scanner. The goal of this thesis was to gain additional knowledge about the use of UAV-based laser scanning for two applications with agriculture and deformation monitoring.

Due to the complex processing, different assessment steps were developed to analyze the point clouds, which are calculated based on direct georeferencing. The separate investigation of the laser scanner only provided new insights, especially in the context of multi-target capability. Finally, development in the use of two applications have shown the potential of UAV-based laser scanning. On the basis of Publications A - E contributing to this thesis, the following main aspects were addressed:

- **Evaluation of direct georeferencing using UAV-based laser scanning**
  The quality of direct georeferencing in UAV-based laser scanning systems can be a limiting factor for different applications. To provide insights about the point cloud quality, four critical aspects were analyzed: point cloud noise, accuracy, precision of repeated measurements, and the influence of different GNSS master stations. The study provided a strategy for point- and parameter-based evaluation and used data from two study areas to evaluate these factors. The methodology involved analyzing point cloud noise by residuals from 3D plane adjustments, which is transferable to nearly every data set. This approach highlighted how noise levels increase with altitude and multiple strip measurements. The strategy for accuracy evaluation compared UAV data against a terrestrial laser scanning (TLS) reference. Furthermore, a new approach for precision analysis using repetitions of a flight plan was introduced with the determination of target-based standard deviation. Finally, the impact of different GNSS master stations was examined by comparing results from an own master station, a CORS station, and two VRS setups. The evaluation showed comparable and reliable results for different master stations. Overall, the study's methodological approach effectively demonstrated how factors like altitude, strip adjustments, and GNSS configuration can influence the quality of direct georeferencing in UAV-based laser scanning systems.

- **Investigation of quality aspects of a full-waveform 2D laser scanner**
  The separation of error sources in UAV-based laser scanning is quite challenging. Therefore, a separate examination focusing on the performance of the laser scanner (e.g., RIEGL miniVUX-2UAV) was proposed. The analysis focused on key parameters like range precision, rangefinder offset, resolution capability, and multi-target capability. The approach and evaluation for the estimation of an intensity-based stochastic model for the range measurement were shown. Furthermore, a measurement setup and analysis of the multi-target capability were presented. It provided a new systematic evaluation of the scanner regarding the capability of separating two objects in a range direction. The study further established a relationship between precision and laser pulse deviation, enhancing the evaluation of future measurements. This relation can be used for the analysis of data sets and the expected precision of multiple echoes. In summary, this analysis provided a comprehensive approach to how 2D laser scanners used in UAV applications could be investigated without the additional errors from the multi-sensor system.

- **Estimation of structural plant traits based on plant height and leaf area index**
  Monitoring the crop status in agriculture through crop parameters is relevant for farmers and breeding applications. One potential is the use of UAV-based laser scanning for the derivation of structural

plant parameters. The analysis within this thesis presented the estimation of structural wheat traits, specifically crop height and plant area index (PAI). One challenge in the processing of point clouds is the classification of soil and plants. This was solved by a novel approach for ground classification incorporating geometric and radiometric features. This method proved to be more effective than traditional approaches, particularly during the early growing phase, providing more accurate ground classification. For crop height estimation, a raster-based method was employed, which showed a strong correlation with manually measured reference heights. However, a systematic error was noted, likely due to the interaction between the laser pulses and the plant canopy, affecting measurements. This is followed by a detailed analysis of the estimation of PAI using the Beer-Lambert law. In summary, this research demonstrated the potential of UAV-based laser scanning for estimating plant traits while addressing challenges related to uncertainties in the process. The novelty and focus of the investigations were the ground classification method and the analysis regarding the accuracy of height and PAI estimation considering the impacting factors.

- **Analysis of UAV-based laser scanning for deformation analysis of a water dam** The second application was the use of UAV-based laser scanning for monitoring a water dam, focusing on overcoming challenges related to trajectory estimation, the special environment, and flight planning. The main contribution involved improving the quality of the point cloud through strip adjustment and validating the results with a TLS reference. The acquisition was performed with a specialized flight pattern with parallel strips at varying altitudes. The investigations showed the challenging trajectory estimation due to the poor satellite geometry, leading to noticeable misalignments between flight strips after direct georeferencing. Building on this point cloud captured at the water dam, an instance segmentation algorithm for stones in a rubble masonry dam was shown as a pre-processing step for deformation monitoring. The instance segmentation methodology involved k-means classification followed by image processing. The first example of using stone instance segmentation was shown with a deformation analysis using the ICP (Iterative Closest Point) algorithm. Overall, this contribution demonstrated the potential of UAV-based laser scanning and the algorithm and use of segmented stone objects for deformation analysis.

In conclusion, this thesis provides detailed insights into the analysis of direct georeferencing in UAV-based laser scanning based on proposed evaluation strategies. The individual study of laser scanner quality provides a better understanding of the sensor used within the multi-sensor system. Finally, the development of methods and analysis in two different applications of precision agriculture and deformation monitoring has shown the potential for the use of UAV-based laser scanning.

In Chapter 6, subsequent research questions following this work were identified. One of the limiting factors, especially in challenging GNSS environments, is the trajectory estimation part. The initial trajectory estimate needs to be improved to increase the quality of point clouds from UAV-based laser scanning. In this context, additional sensors, such as total stations or the combined adjustment of sensor data, including laser scanner measurements, have been identified. Further, an outline of the potential of stone segmentation captured with laser scanning for deformation monitoring was given.

8. List of further publications

This chapter provides an overview of further publications that are not directly related to this thesis and in a few of these publications the author was involved as a co-author.

- Zimmermann, F., Dreier, A., Klingbeil, L., Holst, C., & Kuhlmann, H. (2020). Weniger ist manchmal mehr - Strategien zur Selektion von Satelliten für präzise GNSS-Positionsbestimmungen unter schwierigen Messbedingungen. *In: Wunderlich, T. (Hrsg.): Ingenieurvermessung 20, Beiträge zum 19. Internationalen Ingenieurvermessungskurs, München, Deutschland, Wichmann Verlag, Berlin, Offenbach*, 2020, 177–190
- Dreier, A., Zimmermann, F., Klingbeil, L., Holst, C., & Kuhlmann, H. (2021b). Strategien zur Selektion von Satelliten in kinematischen GNSS-Anwendungen auf Basis von 3D-Umgebungsmodellen. *Allgemeine Vermessungs-Nachrichten (AVN)*, 128 (2021) 1, 13–22
- Klingbeil, L., Dreier, A., Esser, F., Zabawa, L., Pavlic, D., & Kuhlmann, H. (2022). Mobile Mapping auf dem Acker – hochaufgelöste 3D-Vermessung für nachhaltige Pflanzenproduktion. *Allgemeine Vermessungs-Nachrichten (AVN)*, 129 (2022) 3, 96–103
- Tombrink, G., Dreier, A., Klingbeil, L., & Kuhlmann, H. (2023). Trajectory evaluation using repeated rail-bound measurements. *Journal of Applied Geodesy*, 17(3), 205–216
- Cantürk, M., Zabawa, L., Pavlic, D., Dreier, A., Klingbeil, L., & Kuhlmann, H. (2023). UAV-based individual plant detection and geometric parameter extraction in vineyards. *Frontiers in Plant Science*, 14, 1244384
- Dreier, A., Kuhlmann, H., & Klingbeil, L. (2023b). Quality investigation of UAV-based laser scanning with detailed study of multi-target capability. *In: Wieser, A. (Hrsg.): Ingenieurvermessung 23, Beiträge zum 20. Internationalen Ingenieurvermessungskurs, Zurich, Schweiz, Wichmann Verlag, Berlin, Offenbach*, 2023, 235–248
- Dreier, A., Kuhlmann, H., & Klingbeil, L. (2024b). Investigation of quality aspects of UAV-based laser scanning with special focus on multi-target capability. *Allgemeine Vermessungs-Nachrichten (AVN)*, 131 (2024) 2, 67–76
- Grömer, M., Nocerino, E., Calantropio, A., Menna, F., Dreier, A., Winiwarter, L., & Mandlburger, G. (2024). High-detail and low-cost underwater inspection of large-scale hydropower dams. *The International Archives of the Photogrammetry, Remote Sensing and Spatial Information Sciences*, XLVIII-2-2024, 115–120
- Tombrink, G., Dreier, A., Klingbeil, L., & Kuhlmann, H. (2024). Spatio-temporal trajectory alignment for trajectory evaluation. *Journal of Applied Geodesy*, (in publication)

References

Alba, M., Fregonese, L., Prandi, F., Scaioni, M., Valgoi, P., et al. (2006). Structural monitoring of a large dam by terrestrial laser scanning. *International Archives of Photogrammetry, Remote Sensing and Spatial Information Sciences*, 36(5), 6.

Baltsavias, E. P. (1999). Airborne laser scanning: basic relations and formulas. *ISPRS Journal of photogrammetry and remote sensing*, 54(2-3), 199–214.

Barber, D., Mills, J., & Smith-Voysey, S. (2008). Geometric validation of a ground-based mobile laser scanning system. *ISPRS journal of photogrammetry and remote sensing*, 63(1), 128–141.

Bates, J. S., Montzka, C., Schmidt, M., & Jonard, F. (2021). Estimating canopy density parameters time-series for winter wheat using uas mounted lidar. *Remote Sensing*, 13(4), 710.

Becirevic, D., Klingbeil, L., Honecker, A., Schumann, H., Rascher, U., Léon, J., & Kuhlmann, H. (2019). On the derivation of crop heights from multitemporal uav based imagery. *ISPRS Annals of the Photogrammetry, Remote Sensing and Spatial Information Sciences*, IV-2/W5, 95–102.

Boehler, W., Vicent, M. B., Marbs, A., et al. (2003). Investigating laser scanner accuracy. *The International Archives of Photogrammetry, Remote Sensing and Spatial Information Sciences*, 34(Part 5), 696–701.

Brede, B., Lau, A., Bartholomeus, H. M., & Kooistra, L. (2017). Comparing riegl ricopter uav lidar derived canopy height and dbh with terrestrial lidar. *Sensors*, 17(10), 2371.

Cantürk, M., Zabawa, L., Pavlic, D., Dreier, A., Klingbeil, L., & Kuhlmann, H. (2023). UAV-based individual plant detection and geometric parameter extraction in vineyards. *Frontiers in Plant Science*, 14, 1244384.

Cao, L., Liu, H., Fu, X., Zhang, Z., Shen, X., & Ruan, H. (2019). Comparison of uav lidar and digital aerial photogrammetry point clouds for estimating forest structural attributes in subtropical planted forests. *Forests*, 10(2), 145.

Chen, J., Zhu, H., & Li, X. (2016). Automatic extraction of discontinuity orientation from rock mass surface 3d point cloud. *Computers & geosciences*, 95, 18–31.

Coops, N. C., Tompalski, P., Goodbody, T. R., Queinnec, M., Luther, J. E., Bolton, D. K., White, J. C., Wulder, M. A., van Lier, O. R., & Hermosilla, T. (2021). Modelling lidar-derived estimates of forest attributes over space and time: A review of approaches and future trends. *Remote Sensing of Environment*, 260, 112477.

Dalla Corte, A. P., Rex, F. E., Almeida, D. R. A. d., Sanquetta, C. R., Silva, C. A., Moura, M. M., Wilkinson, B., Zambrano, A. M. A., Cunha Neto, E. M. d., Veras, H. F., et al. (2020). Measuring individual tree diameter and height using gatoreye high-density uav-lidar in an integrated crop-livestock-forest system. *Remote Sensing*, 12(5), 863.

Dreier, A., Janßen, J., Kuhlmann, H., & Klingbeil, L. (2021a). Quality analysis of direct georeferencing in aspects of absolute accuracy and precision for a UAV-based laser scanning system. *Remote Sensing*, 13(18), 3564.

Dreier, A., Jost, B., Kuhlmann, H., & Klingbeil, L. (2024a). Investigations of the scan characteristics with special focus on multi-target capability for the 2D laser scanner RIEGL miniVUX-2UAV. *Journal of Applied Geodesy*, 18(1), 97–113.

Dreier, A., Kuhlmann, H., & Klingbeil, L. (2023a). The potential of UAV-based laser scanning for deformation monitoring - case study on a water dam. *5th Joint International Symposium on Deformation Monitoring (JISDM 2022), Editorial Universitat Politècnica de València*, 2023, 261–269.

Dreier, A., Kuhlmann, H., & Klingbeil, L. (2023b). Quality investigation of UAV-based laser scanning with detailed study of multi-target capability. *In: Wieser, A. (Hrsg.): Ingenieurvermessung 23, Beiträge zum 20. Internationalen Ingenieurvermessungskurs, Zurich, Schweiz, Wichmann Verlag, Berlin, Offenbach*, 2023, 235–248.

Dreier, A., Kuhlmann, H., & Klingbeil, L. (2024b). Investigation of quality aspects of UAV-based laser scanning with special focus on multi-target capability. *Allgemeine Vermessungs-Nachrichten (AVN)*, 131 (2024) 2, 67–76.

Dreier, A., Lopez, G., Bajracharya, R., Kuhlmann, H., & Klingbeil, L. (2025a). Structural wheat trait estimation using UAV-based laser scanning data: Analysis of critical aspects and recommendations based on a case study. *Precision Agriculture*, 26(18).

Dreier, A., Tobies, A., Kuhlmann, H., & Klingbeil, L. (2025b). Stone instance segmentation of rubble masonry based on laser scanning point clouds. *Measurement*, 242, 115905.

Dreier, A., Zimmermann, F., Klingbeil, L., Holst, C., & Kuhlmann, H. (2021b). Strategien zur Selektion von Satelliten in kinematischen GNSS-Anwendungen auf Basis von 3D-Umgebungsmodellen. *Allgemeine Vermessungs-Nachrichten (AVN)*, 128 (2021) 1, 13–22.

Fang, H., Baret, F., Plummer, S., & Schaepman-Strub, G. (2019). An overview of global leaf area index (lai): Methods, products, validation, and applications. *Reviews of Geophysics*, 57(3), 739–799.

Galanakis, D., Maravelakis, E., Pocobelli, D. P., Vidakis, N., Petousis, M., Konstantaras, A., & Tsakoumaki, M. (2023). Svd-based point cloud 3d stone by stone segmentation for cultural heritage structural analysis – the case of the apollo temple at delphi. *Journal of Cultural Heritage*, 61, 177–187.

Glennie, C. (2007). Rigorous 3d error analysis of kinematic scanning lidar systems. *Journal of Applied Geodesy*, (1), 147–157.

Glira, P. (2018). *Hybrid orientation of LiDAR point clouds and aerial images*. PhD thesis, Technische Universität Wien.

Gräfe, G. (2009). *Kinematische Anwendungen von Laserscannern im Straßenraum*. PhD thesis, Univ. der Bundeswehr München, Fak. für Bauingenieur- und Vermessenswesen.

Grömer, M., Nocerino, E., Calantropio, A., Menna, F., Dreier, A., Winiwarter, L., & Mandlburger, G. (2024). High-detail and low-cost underwater inspection of large-scale hydropower dams. *The International Archives of the Photogrammetry, Remote Sensing and Spatial Information Sciences*, XLVIII-2-2024, 115–120.

Guan, H., Li, J., Cao, S., & Yu, Y. (2016). Use of mobile lidar in road information inventory: A review. *International Journal of Image and Data Fusion*, 7(3), 219–242.

Guimarães, N., Pádua, L., Marques, P., Silva, N., Peres, E., & Sousa, J. J. (2020). Forestry remote sensing from unmanned aerial vehicles: A review focusing on the data, processing and potentialities. *Remote Sensing*, 12(6), 1046.

Habib, A., Bang, K. I., Kersting, A. P., & Lee, D.-C. (2009). Error budget of lidar systems and quality control of the derived data. *Photogrammetric Engineering & Remote Sensing*, 75(9), 1093–1108.

Heinz, E., Mettenleiter, M., Kuhlmann, H., & Holst, C. (2018). Strategy for determining the stochastic distance characteristics of the 2d laser scanner z+ f profiler 9012a with special focus on the close range. *Sensors*, 18(7), 2253.

Heinz, E. E. (2021). *Beiträge zur Kalibrierung und Evaluierung von Multisensorsystemen für kinematisches Laserscanning*. PhD thesis, Universitäts- und Landesbibliothek Bonn.

Hesse, C. (2008). *Hochauflösende kinematische Objekterfassung mit terrestrischen Laserscannern*. PhD thesis, Leibniz-Univ., Fachrichtung Geodäsie und Geoinformatik.

Huxhagen, U., Kern, F., & Siegrist, B. (2011). Untersuchung zum auflösungsvermögen terrestrischer laserscanner mittels böhler-stern. *DGPF Tagungsband*, 20(2011), 409–418.

Janßen, J., Medic, T., Kuhlmann, H., & Holst, C. (2019). Decreasing the uncertainty of the target center estimation at terrestrial laser scanning by choosing the best algorithm and by improving the target design. *Remote Sensing*, 11(7), 845.

Jóźków, G., Walicka, A., & Borkowski, A. (2021). Monitoring terrain deformations caused by underground mining using uav data. *The International Archives of the Photogrammetry, Remote Sensing and Spatial Information Sciences*, 43, 737–744.

Kaartinen, H., Hyyppä, J., Kukko, A., Jaakkola, A., & Hyyppä, H. (2012). Benchmarking the performance of mobile laser scanning systems using a permanent test field. *Sensors*, 12(9), 12814–12835.

Klingbeil, L., Dreier, A., Esser, F., Zabawa, L., Pavlic, D., & Kuhlmann, H. (2022). Mobile Mapping auf dem Acker – hochaufgelöste 3D-Vermessung für nachhaltige Pflanzenproduktion. *Allgemeine Vermessungs-Nachrichten (AVN)*, 129 (2022) 3, 96–103.

Krinner, G., Viovy, N., de Noblet-Ducoudré, N., Ogée, J., Polcher, J., Friedlingstein, P., Ciais, P., Sitch, S., & Prentice, I. C. (2005). A dynamic global vegetation model for studies of the coupled atmosphere-biosphere system. *Global Biogeochemical Cycles*, 19(1).

Kukko, A., Kaartinen, H., Hyyppä, J., & Chen, Y. (2012). Multiplatform mobile laser scanning: Usability and performance. *Sensors*, 12(9), 11712–11733.

Lague, D., Brodu, N., & Leroux, J. (2013). Accurate 3d comparison of complex topography with terrestrial laser scanner: Application to the rangitikei canyon (n-z). *ISPRS Journal of Photogrammetry and Remote Sensing*, 82, 10–26.

Lei, L., Qiu, C., Li, Z., Han, D., Han, L., Zhu, Y., Wu, J., Xu, B., Feng, H., Yang, H., et al. (2019). Effect of leaf occlusion on leaf area index inversion of maize using uav–lidar data. *Remote Sensing*, 11(9), 1067.

Lim, S., Thatcher, C. A., Brock, J. C., Kimbrow, D. R., Danielson, J. J., & Reynolds, B. (2013). Accuracy assessment of a mobile terrestrial lidar survey at padre island national seashore. *International journal of remote sensing*, 34(18), 6355–6366.

Mallet, C. & Bretar, F. (2009). Full-waveform topographic lidar: State-of-the-art. *ISPRS Journal of photogrammetry and remote sensing*, 64(1), 1–16.

Mandlburger, G. (2022a). UAV laser scanning. *In: Eltner, A. et al. (Eds.): UAVs for the Environmental Sciences. wbg, Darmstadt*, (pp. 199–217).

Mandlburger, G. (2022b). *UAV laser scanning, In A. Eltner, D. Hoffmeister, A. Kaiser, P. Karrasch, L. Klingbeil, C. Stöcker, & A. Rovere (Eds.), UAVs for the Environmental Sciences - Methods and Applications (pp. 199–217).* Darmstadt: wbg (Wissenschaftliche Buchgesellschaft).

Mandlburger, G., Pfennigbauer, M., Schwarz, R., Flöry, S., & Nussbaumer, L. (2020a). Concept and performance evaluation of a novel uav-borne topobathymetric lidar sensor. *Remote Sensing*, 12(6), 986.

Mandlburger, G., Pfennigbauer, M., Schwarz, R., Flöry, S., & Nussbaumer, L. (2020b). Concept and performance evaluation of a novel UAV-borne topo-bathymetric lidar sensor. *Remote Sensing*, 12(6).

Martin, D. & Gatta, G. (2006). Calibration of total stations instruments at the esrf. In *Proceedings of XXIII FIG Congress (2006)* (pp. 1–14).

Medić, T. (2021). *Efficient calibration strategies for panoramic terrestrial laser scanners*. PhD thesis, University of Bonn, Bonn, Germany.

Moudrỳ, V., Gdulová, K., Fogl, M., Klápště, P., Urban, R., Komárek, J., Moudrá, L., Štroner, M., Barták, V., & Solskỳ, M. (2019). Comparison of leaf-off and leaf-on combined uav imagery and airborne lidar for assessment of a post-mining site terrain and vegetation structure: Prospects for monitoring hazards and restoration success. *Applied geography*, 104, 32–41.

Perez-Harguindeguy, N., Diaz, S., Garnier, E., Lavorel, S., Poorter, H., Jaureguiberry, P., Bret-Harte, M. S., Cornwell, W. K., Craine, J. M., Gurvich, D. E., et al. (2016). Corrigendum to: New handbook for standardised measurement of plant functional traits worldwide. *Australian Journal of botany*, 64(8), 715–716.

Pfeifer, N., Mandlburger, G., Otepka, J., & Karel, W. (2014). Opals – a framework for airborne laser scanning data analysis. *Computers, Environment and Urban Systems*, 45, 125–136.

Pfennigbauer, M. & Ullrich, A. (2010). Improving quality of laser scanning data acquisition through calibrated amplitude and pulse deviation measurement. In *Laser Radar Technology and Applications XV*, volume 7684 (pp. 463–472).: SPIE.

Pilarska, M., Ostrowski, W., Bakuła, K., Górski, K., & Kurczyński, Z. (2016). The potential of light laser scanners developed for unmanned aerial vehicles-the review and accuracy. *International Archives of the Photogrammetry, Remote Sensing & Spatial Information Sciences*, 42.

Pöppl, F., Ullrich, A., Mandlburger, G., & Pfeifer, N. (2024). A flexible trajectory estimation methodology for kinematic laser scanning. *ISPRS Journal of Photogrammetry and Remote Sensing*, 215, 62–79.

Pöppl, F., Neuner, H., Mandlburger, G., & Pfeifer, N. (2023). Integrated trajectory estimation for 3d kinematic mapping with gnss, ins and imaging sensors: A framework and review. *ISPRS Journal of Photogrammetry and Remote Sensing*, 196, 287–305.

RIEGL Laser Measurement Systems GmbH (2020). RIEGL miniVUX-SYS Data Sheet. `http://www.riegl.com/uploads/tx_pxpriegldownloads/RIEGL_miniVUX-SYS_Datasheet_2022-09-27_03.pdf`. [Online; accessed 17-November-2022].

RIEGL Laser Measurement Systems GmbH (2021). RIEGL miniVUX-2UAV Data Sheet. [accessed 21-April-2021].

Roth, L., Aasen, H., Walter, A., & Liebisch, F. (2018). Extracting leaf area index using viewing geometry effects—a new perspective on high-resolution unmanned aerial system photography. *ISPRS Journal of Photogrammetry and Remote Sensing*, 141, 161–175.

Scaioni, M., Marsella, M., Crosetto, M., Tornatore, V., & Wang, J. (2018). Geodetic and remote-sensing sensors for dam deformation monitoring. *Sensors*, 18(11), 3682.

Schlichting, A., Brenner, C., & Schön, S. (2014). Bewertung von inertial/gnss-modulen mittels laserscannern und bekannter landmarken. *PFG Photogrammetrie, Fernerkundung, Geoinformation*, (pp. 5–15).

Schmitz, B., Holst, C., Medic, T., Lichti, D. D., & Kuhlmann, H. (2019). How to efficiently determine the range precision of 3D terrestrial laser scanners. *Sensors*, 19(6).

Schmitz, B., Kuhlmann, H., & Holst, C. (2020). Investigating the resolution capability of terrestrial laser scanners and its impact on the effective number of measurements. *ISPRS Journal of Photogrammetry and Remote Sensing*, 159, 41–52.

Shahmoradi, J., Talebi, E., Roghanchi, P., & Hassanalian, M. (2020). A comprehensive review of applications of drone technology in the mining industry. *Drones*, 4(3), 34.

Shan, J. & Toth, C. K. (2018). *Topographic laser ranging and scanning: principles and processing.* CRC press.

Solberg, S., Næsset, E., Hanssen, K. H., & Christiansen, E. (2006). Mapping defoliation during a severe insect attack on scots pine using airborne laser scanning. *Remote Sensing of Environment*, 102(3), 364–376.

Stöcker, C., Nex, F., Koeva, M., & Gerke, M. (2017). Quality assessment of combined imu/gnss data for direct georeferencing in the context of uav-based mapping. *The International Archives of the Photogrammetry, Remote Sensing and Spatial Information Sciences*, 42, 355–361.

Storm, H., Seidel, S. J., Klingbeil, L., Ewert, F., Vereecken, H., Amelung, W., Behnke, S., Bennewitz, M., Börner, J., Döring, T., Gall, J., Mahlein, A.-K., McCool, C., Rascher, U., Wrobel, S., Schnepf, A., Stachniss, C., & Kuhlmann, H. (2024). Research priorities to leverage smart digital technologies for sustainable crop production. *European Journal of Agronomy*, 156, 127178.

Tombrink, G., Dreier, A., Klingbeil, L., & Kuhlmann, H. (2023). Trajectory evaluation using repeated rail-bound measurements. *Journal of Applied Geodesy*, 17(3), 205–216.

Tombrink, G., Dreier, A., Klingbeil, L., & Kuhlmann, H. (2024). Spatio-temporal trajectory alignment for trajectory evaluation. *Journal of Applied Geodesy*, (in publication).

Toschi, I., Rodríguez-Gonzálvez, P., Remondino, F., Minto, S., Orlandini, S., & Fuller, A. (2015). Accuracy evaluation of a mobile mapping system with advanced statistical methods. *The International Archives of Photogrammetry, Remote Sensing and Spatial Information Sciences*, 40(5), 245.

Tucci, G., Visintini, D., Bonora, V., & Parisi, E. I. (2018). Examination of indoor mobile mapping systems in a diversified internal/external test field. *Applied Sciences*, 8(3), 401.

Tulldahl, H. M., Bissmarck, F., Larsson, H., Grönwall, C., & Tolt, G. (2015). Accuracy evaluation of 3d lidar data from small uav. In *Electro-Optical Remote Sensing, Photonic Technologies, and Applications IX*, volume 9649 (pp. 964903).: International Society for Optics and Photonics.

Ullrich, A. & Pfennigbauer, M. (2011). Echo digitization and waveform analysis in airborne and terrestrial laser scanning. In *Photogrammetric week*, volume 11 (pp. 217–228).

Wang, G., Li, P., Li, Z., Ding, D., Qiao, L., Xu, J., Li, G., & Wang, H. (2020). Coastal dam inundation assessment for the yellow river delta: Measurements, analysis and scenario. *Remote sensing*, 12(21), 3658.

Wang, Y. & Fang, H. (2020). Estimation of lai with the lidar technology: A review. *Remote Sensing*, 12(20), 3457.

Wiedemann, W. & Holst, C. (2023). Identifying individual rocks within laser scans for a rigorous deformation analysis of water dams. In *5th Joint International Symposium on Deformation Monitoring (JISDM 2022)* (pp. 327–334).: Editorial Universitat Politècnica de València.

Winiwarter, L., Anders, K., Wujanz, D., & Höfle, B. (2020). Influence of ranging uncertainty of terrestrial laser scanning on change detection in topographic 3D point clouds. *ISPRS Annals of the Photogrammetry, Remote Sensing and Spatial Information Sciences*, 2, 789–796.

Wujanz, D., Burger, M., Tschirschwitz, F., Nietzschmann, T., Neitzel, F., & Kersten, T. P. (2018). Determination of intensity-based stochastic models for terrestrial laser scanners utilising 3D-point clouds. *Sensors*, 18(7).

Xu, H., Li, H., Yang, X., Qi, S., & Zhou, J. (2018). Integration of terrestrial laser scanning and nurbs modeling for the deformation monitoring of an earth-rock dam. *Sensors*, 19(1), 22.

Yan, G., Hu, R., Luo, J., Weiss, M., Jiang, H., Mu, X., Xie, D., & Zhang, W. (2019). Review of indirect optical measurements of leaf area index: Recent advances, challenges, and perspectives. *Agricultural and forest meteorology*, 265, 390–411.

Yang, S., Hou, M., & Li, S. (2023). Three-dimensional point cloud semantic segmentation for cultural heritage: a comprehensive review. *Remote Sensing*, 15(3), 548.

Zhang, W., Qi, J., Wan, P., Wang, H., Xie, D., Wang, X., & Yan, G. (2016). An easy-to-use airborne lidar data filtering method based on cloth simulation. *Remote sensing*, 8(6), 501.

Zieher, T., Bremer, M., Rutzinger, M., Pfeiffer, J., Fritzmann, P., & Wichmann, V. (2019). Assessment of landslide-induced displacement and deformation of above-ground objects using uav-borne and airborne laser scanning data. *ISPRS Annals of the Photogrammetry, Remote Sensing and Spatial Information Sciences*, 4, 461–467.

Zimmermann, F., Dreier, A., Klingbeil, L., Holst, C., & Kuhlmann, H. (2020). Weniger ist manchmal mehr - Strategien zur Selektion von Satelliten für präzise GNSS-Positionsbestimmungen unter schwierigen Messbedingungen. *In: Wunderlich, T. (Hrsg.): Ingenieurvermessung 20, Beiträge zum 19. Internationalen Ingenieurvermessungskurs, München, Deutschland, Wichmann Verlag, Berlin, Offenbach*, 2020, 177–190.